Proyecto Fin de Master

Máster Universitario en Ingeniería Aeronáutica

# MECHANICAL ASSESSMENT OF THE SUPPORTS FOR THE TOROIDAL FIELD COILS OF A TOKAMAK

Autor: José Manuel Cubero Vállez

Tutor: Juan Manuel Ayllón-Guerola

Tutor ponente: Carlos Navarro Pintado

**Dpto. Ingeniería Mecánica y Fabricación**
**Escuela Técnica Superior de Ingeniería**
**Universidad de Sevilla**

Sevilla, 2019

Proyecto Fin de Master

Máster Universitario en Ingeniería Aeronáutica

# MECHANICAL ASSESSMENT OF THE SUPPORTS FOR THE TOROIDAL FIELD COILS OF A TOKAMAK

Autor:

José Manuel Cubero Vállez

Tutor:

Juan Manuel Ayllón-Guerola

Tutor ponente:

Carlos Navarro Pintado

Dpto. de Ingeniería Mecánica y Fabricación

Escuela Técnica Superior de Ingeniería

Universidad de Sevilla

Sevilla, 2019

Proyecto Fin de Máster:

MECHANICAL ASSESSMENT OF THE SUPPORTS FOR THE TOROIDAL FIELD COILS
OF A TOKAMAK

| | |
|---|---|
| Autor: | José Manuel Cubero Vállez |
| Tutores: | Juan Manuel Ayllón -Guerola |
| Tutor ponente: | Carlos Navarro Pintado |

El tribunal nombrado para juzgar el Proyecto arriba indicado, compuesto por los siguientes miembros:

Presidente:

Vocales:

Secretario:

Acuerdan otorgarle la calificación de:

Sevilla, 2019

El Secretario del Tribunal

# Agradecimientos

Aprovecho este espacio para agradecer a todas las personas que se toparon conmigo durante mi vida académica, ya sean amigos, profesores o sencillamente compañeros de clase y trabajos, ya que cada uno, a su manera, con su forma de actuar, influyeron en mi de miles de formas distintas, positiva o negativamente, ayudando, o complicándolo todo mucho más, ya que ahora forman parte de mí, de mi experiencia y de lo que me he convertido en este viaje que empezó en aquel mes de septiembre de 2009 a los 18 años.

Gracias en especial a aquellos amigos más cercanos, que estuvieron ahí en las largas tardes de biblioteca, en las infinitas madrugadas de estudio y en las intensas épocas de exámenes. Sin ellos, todo hubiera sido mucho más costoso, y, por supuesto, menos divertido.

Y, por último y más importante, gracias a mis padres, que se pasaron la vida trabajando para darme la oportunidad de estudiar una carrera cuando ellos nunca la tuvieron, que nunca me presionaron en las malas épocas y que estuvieron siempre ahí para apoyarme cuando era necesario. Su firma no estará en el diploma, pocas injusticias mayores que esta veré a lo largo de mi vida.

*José Manuel Cubero Vállez*
*Ingeniero Aeronáutico*
*Sevilla, 2019*

# INDEX

# ILLUSTRATIONS INDEX

# 1 Introduction

## 1.1 Nuclear fusion

Nowadays, the energy consumption by the industry and the world population is in continuously increase. Although there are currently some investigations and researches of renewable energies and its storage, it is probable that they will not be enough to cover the actual consumption and we will need a different energy source. Nowadays, this different source comes from the fossil fuels, however, it is being working in a future in which the alternative could be the nuclear energy. This is due because the continuous use fossil fuels (limited on Earth), with their related $CO_2$ emissions are destroying our planet.

On the other hand, the nuclear fusion reactions generate very danger wastes that can be disintegrated in about 50 years, a time that can seem very long, but irrelevant if we compare with the disintegration of other materials used by the humans as the plastic or the glass.

A nuclear fusion reaction is the combination of nuclei of small elements to form a new bigger one under controlled conditions and get power gain from this action. This power generated is much more (about million times) than the energy obtained by combining the same elements chemically. The cause of this energy release is because the final mass of the element is less than the sum of the components. This difference is, therefore, converted to energy as described by Einstein's equation:

$$E = m * c^2$$

In order to produce fusion reactions, the nuclei must overcome the Coulomb repulsion barrier to reach the nuclear potential, where they can combine to form a heavy nucleus, which then decays in nuclei and particle whose total mass is less than the mass of the interacting nuclei.

To achieve this, it is necessary to expose the elements to a very high temperature in order to get high relative velocities large enough to overcome the Coulomb barrier. At these high temperatures, the gas is ionized (plasma state), macroscopically neutral but formed of electrically charged particles, which allows to confine them with magnetic fields. The fusion reactions in hot plasma are known as thermonuclear reactions. For these reactions, one of the main conditions is that the power generated in the reactor must be enough to replace the loss of power from the plasma, and it is called the "Lawson Criterion".

The probability of two elements to fusion comes from the effective section, as larger as it will be, larger is the chance to the joint of the nuclei. It depends on the energy and type of the particle as seen in Figure 1.
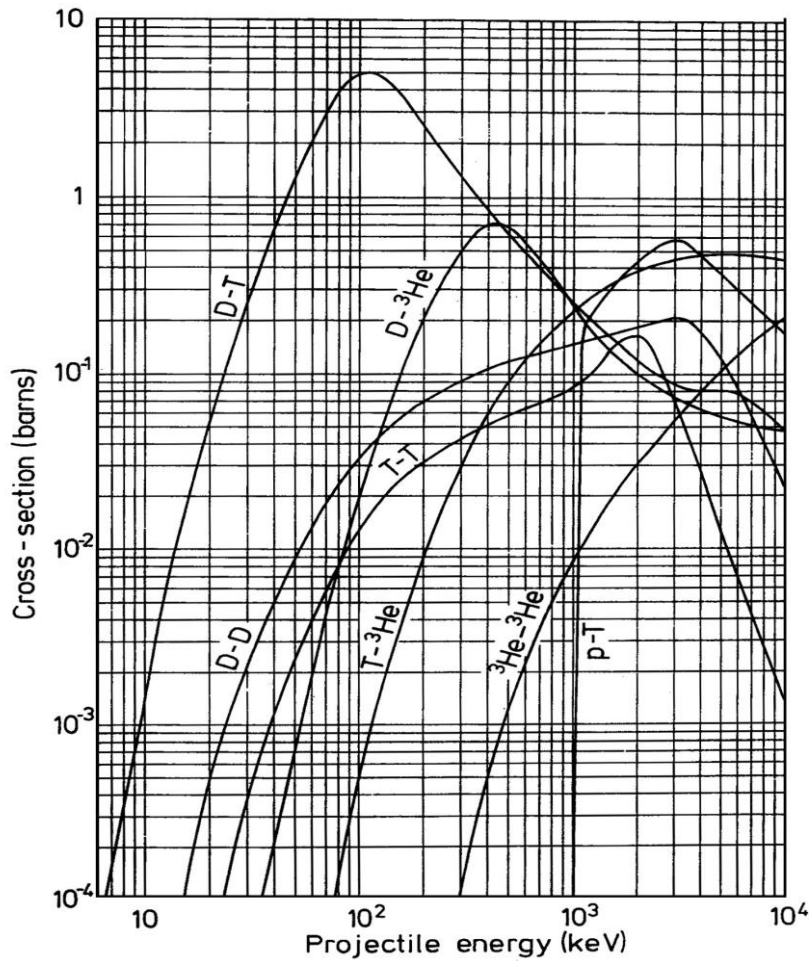
*Figure 1 - Effective Section*

Nowadays, the most promising reaction is the fusion of deuterium and tritium (D-T) (isotopes of hydrogen). For it, the "Lawson criterion" states that the product of the particle density (n) and the confinement time $\tau_E$:

$$n * \tau_E > 2 - 3 * 10^{20} \ m^{-3}s$$

and that the breakeven condition, necessary to achieve the reaction is:

$$n * T * \tau_E > 5 * 10^{21} \ KeVm^{-3}s$$

where T is the temperature.

One of the positive points of this reaction is that the materials used (deuterium and tritium) are abundant in the Earth. The deuterium can be obtained from the sea water where there is approximately a concentration of 100 mg of deuterium per each 3 L of water.

On the other hand, the quantity of tritium is much less than the deuterium, and it is radioactive, which means that it tends to disintegrate itself. Anyway, we can get it from a lithium isotope ($^6$Li) that is found in the 7.5% of the natural lithium.

The plasma of sufficient density must be heated to high temperatures and confined time enough to achieve fusion reaction. There are three main mechanisms to confine these hot plasmas:

2

### 1.  Magnetic confinement (see Figure 2)

It is based on the use of magnetic fields, typically over 100.000 times the magnetic field of the Earth, arranged in a configuration to prevent the charged particles leaking out, called "magnetic bottle" in which the electrically charged particles will follow the magnetic lines. It is usually considered more promising for practical power production nowadays. For more information, refer to Magnetic confinement section.
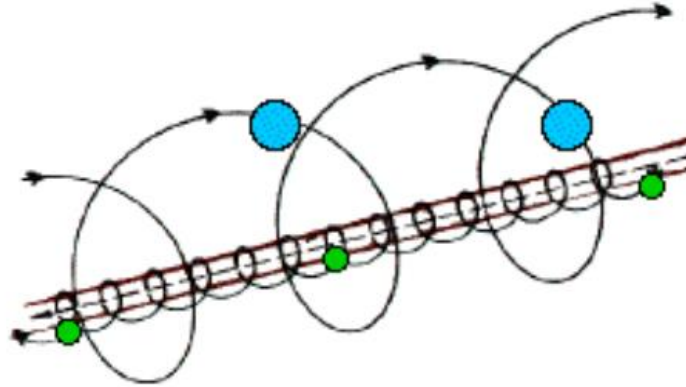


*Figure 2 - Magnetic Confinement*

### 2.  Inertial confinement (see Figure 3)

It is based on the use of powerful lasers or high energy particle beams to compress the fusion fuel. Generally, the systems use a single laser, the *driver*, whose beam is split up into a number of beams, which are subsequently individually amplified by a trillion times or more, that are sent into the reaction chamber. The heat applied by the driver causes the outer layer of the target to explode.

The material exploding off the surface causes the remaining material on the inside to be driven inwards with great force, eventually collapsing into a tiny near-spherical ball. In modern devices the density of the resulting fuel mixture is as much as one-hundred times the density of lead, around 1000 g/cm³. This density is not high enough to create any useful rate of fusion on its own. However, during the collapse of the fuel, shock waves also form and travel into the centre of the fuel at high speed. When they meet their counterparts moving in from the other sides of the fuel in the centre, the density of that spot is raised much further.



*Figure 3 - Inertial Confinement*

### 3. Gravitational confinement (see Figure 4)

The force of gravity is able to confine the fuel. However, the mass needed is so great that it cannot be achieved in a laboratory, only in some big stars as the sun. In them, after the supply of hydrogen is exhausted in their cores, their cores (or a shell around the core) start fusing helium to carbon. In the most massive stars (at least 8–11 solar masses), the process co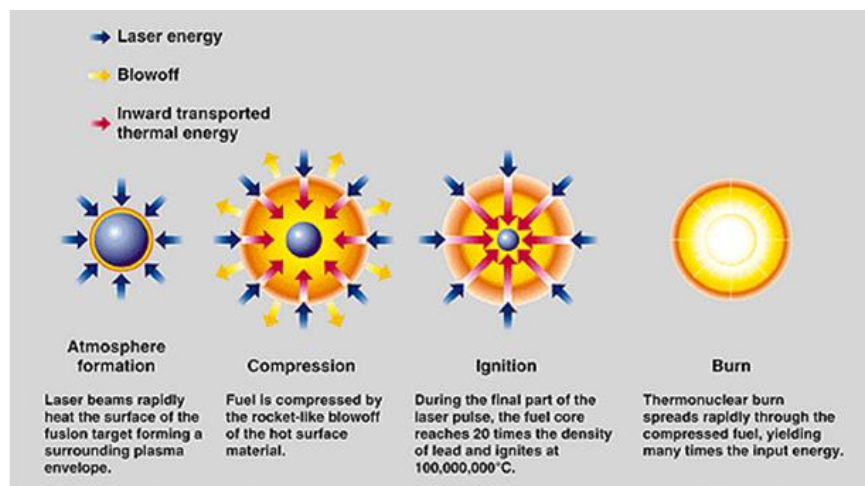ntinues until some of their energy is produced by fusing lighter elements to iron. As iron has one of the highest binding energies, reactions producing heavier elements are generally endothermic.

Therefore significant amounts of heavier elements are not formed during stable periods of massive star evolution, but are formed in supernova explosions. Some lighter stars also form these elements in the outer parts of the stars over long periods of time, by absorbing energy from fusion in the inside of the star, by absorbing neutrons that are emitted from the fusion process.
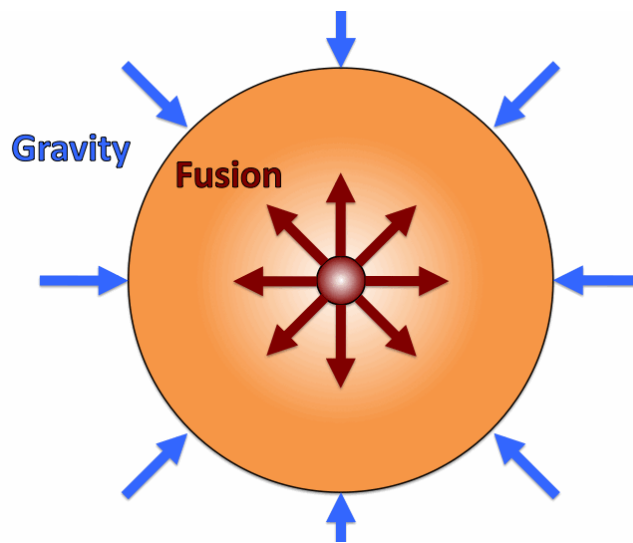


*Figure 4 - Gravitational Confinement*

The magnetic confinement is the one which has shown very significant progress and it is a serious candidate for future fusion reactors.

## 1.2   Magnetic confinement

As the plasma consist of charged particles, the magnetic fields can be used to confine the plasma in perpendicular directions to the magnetic field lines.

A simple example of a magnetic confinement system is a long solenoid which force to the particles to go around the axial field avoiding the particle motion in the perpendicular direction to the magnetic field.

However, this example is not good enough as a magnetic confinement system, due to the particles could leak out from the solenoid extremes (see Figure 2), which provoke a confinement time limit. A simple way of preventing this axial leakage would be to have a long solenoid without extremes, which can be done if we convert it into a torus, thus making it endless (see Figure 5).

*Figure 5 - Magnetic Confinement in a Torus*

It would be thought that the particles will keep the motion around the torus and will be confined while describing a helical trajectory around the magnetic field lines. However, it is demonstrated that the magnetic field in this system has gradients as well as curvature and net effect of these is that charged particles, in addition to gyration and axial motion also acquire a drift across the magnetic field. These drifts are in opposite directions for electrons and ions and result in a ver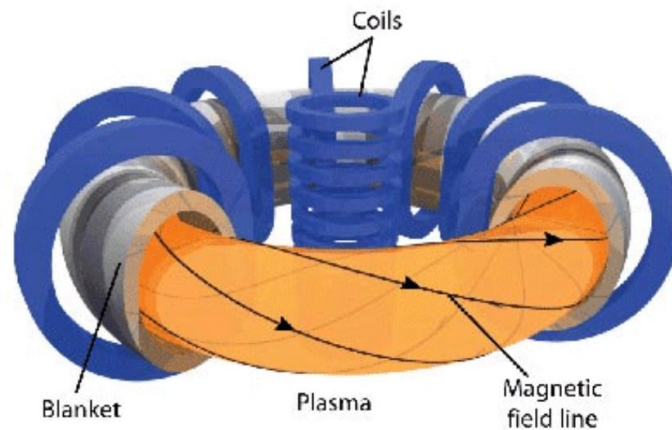tical polarization of the electric field, which results in plasma getting thrown out across the magnetic field in radial direction and the confinement will be lost.

So, a pure toroidal magnetic field system is not able to confine the plasma. One of the typical techniques to do this is to add a poloidal magnetic field to the toroidal one, which results in helical magnetic field lines that some particles can go through.

The device which deploys toroidal current for producing the poloidal magnetic field is the Tokamak. This name comes from the acronym of the russian word "ToroidaInya Kamera Magnetnaya Katushka" which means "the toroidal chamber in magnetic field".

The tokamak employs many magnetic fields to ensure the plasma stays tightly confined and away from its walls. The plasma must be dense for fusion to occur, but the temperature of the plasma gets so high that anything it touches would melt instantly. This is why extremely strong magnets are needed to keep it away from the tokamak walls. Current tokamaks use two magnetic fields, a poloidal and a toroidal one. The poloidal field is created from the transformer effect and the current in the plasma itself. This field causes the plasma particles to spin in a helix pattern as it travels through the tokamak. This spinning keeps the particles constantly moving toward the centre of the toroidal field and away from the walls. This Figure 6 helps to show this effect.
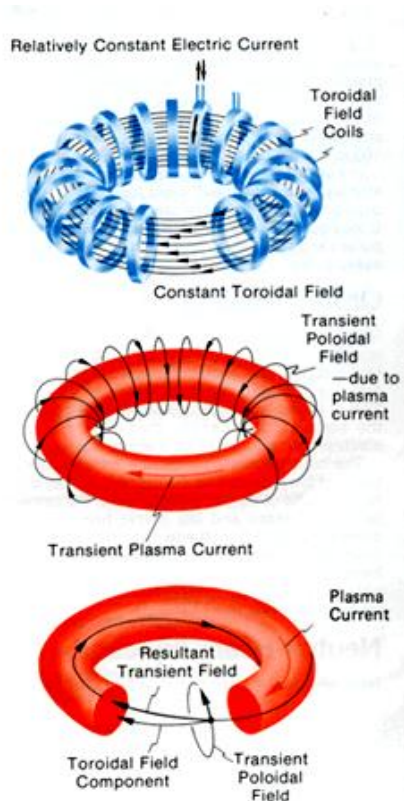
*Figure 6 - Torus Magnetic Confinement*

Magnets lining the walls of the toroid shaped tokamak produce the toroidal field. Magnets wrapped around the outside of the toroid vertically produce a field that travels horizontally throughout the torus. This keeps the plasma flowing through the inside of the tokamak and keeps it away from the side walls because the field always points straight horizontally (see Figure 7).
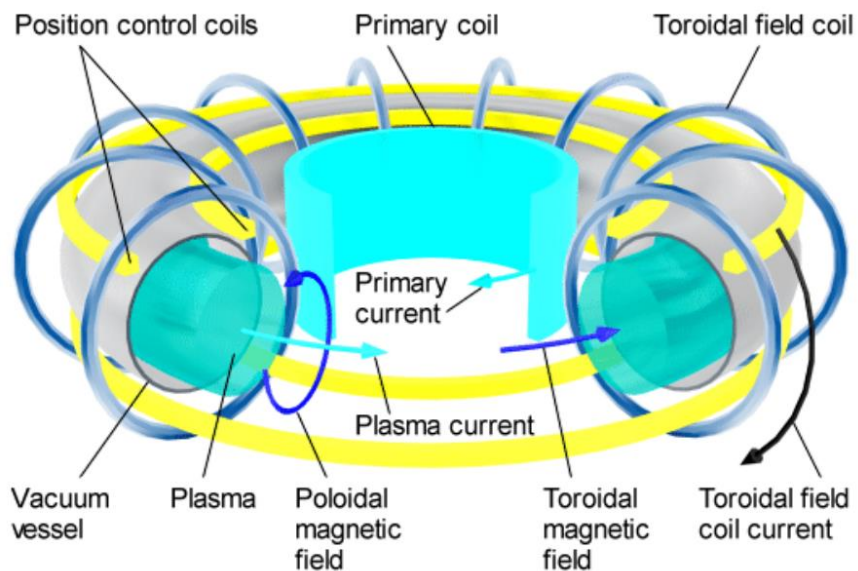


*Figure 7 - Tokamak Magnetic Confinement*

## 1.3   The Tokamak

A tokamak is a device that uses a powerful magnetic field to confine a hot plasma in the shape of a torus. The tokamak is one of several types of magnetic confinement devices that are being developed to produce controlled thermonuclear fusion power. Nowadays, it is the principal candidate for a fusion reactor.

Regarding the way to magnetically confine the plasma in a tokamak, the magnetic field lines follow a helical trajectory around the torus. The toroidal component of this magnetic field is produced by toroidal field coils, whereas the poloidal component is generated by an electric current inside the plasma, which travels around the torus. This current is induced in the plasma by a central solenoid, in an identical way to the induced current in the secondary coil of a transformer, during a finite time interval. Additionally, poloidal field coils are used for plasma positioning and shaping. See Figure 8 to obtain more details about the tokamak configuration.
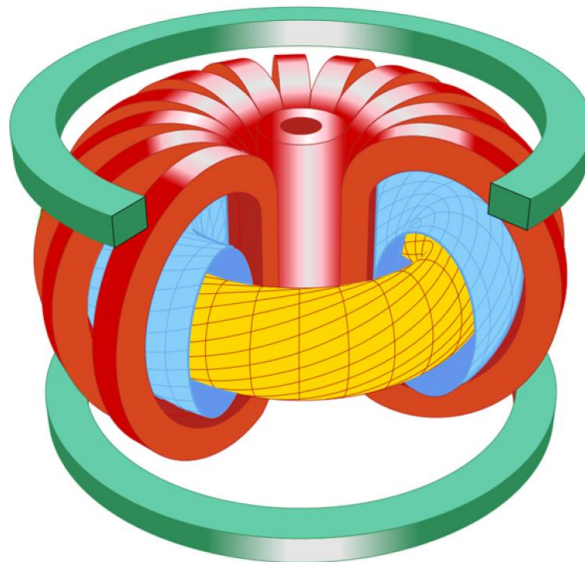


*Figure 8 - Color Scheme of the Tokamak Concept*

The first theoretical idea of a tokamak comes from the 1950s. This idea was developed by Igor Tamm and Andrei Sakharov based on a letter written by Oleg Lavrentiev. This letter outlined the idea of using an atomic bomb to ignite a fusion fuel, and then went on to describe a system that used electrostatic fields to contain a hot plasma in a steady state for energy production.

Anyway, the first tokamak considered as it was the T-1, attributed to Natan Yavlinskii in 1958. It demonstrated that a stable plasma equilibrium requires magnetic field lines that wind around the torus in a helix.

During the 1960s, a lot of work was done on the project. And, by the end of the decade, the performance results of the T-1 were released (confirmed by some United Kingdom experts), which made that this technology started to be taken in account.

This progress made that there were dozens of tokamaks in use around the world by the mid-1970s as, for example, T-15 in the Soviet Union, Joint European Torus (JET) in Europe, Tokamak Fusion Test Reactor (TFTR) in the United States and JT-60 in Japan.

Over the years, there have been many countries which decided to develop his own tokamak (more than one in many cases). The Table 1 includes those that are still operational with the year of the first operation:

| Year | Name | Country |
|------|------|---------|
| 1960 | TM1-MH (renamed to Castor in 1977 and to Golem in 2007) | Czech Republic |
| 1975 | T-10 | Russia |
| 1983 | JET | United Kingdom |
| 1986 | DIII-D | United States |
| 1987 | STOR-M | Canada |
| 1988 | Tore Supra | France |
| 1989 | Aditya | India |
| 1989 | COMPASS | Czech Republic (previously in UK) |
| 1990 | FTU | Italy |
| 1991 | ISTTOK | Portugal |
| 1991 | ASDEX | Germany |
| 1992 | H-1NF | Australia |
| 1992 | TCV | Switzerland |
| 1994 | TCABR | Brazil (previously in Switzerland) |
| 1995 | HT-7 | China |
| 1996 | Pegasus | United States |
| 1999 | NSTX | United States |
| 1999 | Globus-M | Russia |
| 2002 | HL-2A | China |
| 2006 | EAST (HT-7U) | China |
| 2008 | KSTAR | South Korea |
| 2010 | JT-60SA | Japan |
| 2012 | Medusa CR | Costa Rica |
| 2012 | SST-1 | India |
| 2012 | IR-T1 | Iran |
| 2015 | ST25-HTS | United Kingdom |
| 2017 | KTM | Kazakhstan |
| 2018 | ST40 | United Kingdom |

*Table 1 - Operational Tokamaks*

However, the most of them generated problems that limited their performance. Solving them required a much larger and more expensive machine that needed the cooperation between many countries. Then, in November 1985, Ronald Reagan and Mikhail Gorbachov made an agreement to start the project of the ITER (International Thermonuclear Experimental Reactor) with the equal participation of the Soviet Union, the European Atomic Energy Community, the United States and Japan.

Nowadays, the project is run by the European Union, India, Japan, China, Russia (old Soviet Union), South Korea and the United States and it is expected to be assembled and working (first plasma) in 2025. The target is to produce a fusion plasma equivalent to 500 MW (megawatts) of thermal output power for around twenty minutes while 50 megawatts of thermal power are injected into the tokamak.

# 2 Problem definition

The scope of this project is to calculate the shape and dimension of the supports for the toroidal field coils of a tokamak in order to resist the different forces generated by the magnetic field needed for its operation.

As there are a lot of different shapes and geometries for tokamaks, for this work, the VEST cylindrical tokamak has been taken as a reference [1]. The idea is to develop a systematic methodology that allows the calculation of the forces that the supports need to withstand. Then, with these forces calculated, use them for the dimensioning of the supports for the toroidal field coils as an example of its application. The methodology developed here could be easily adapted for designing other structural elements in the tokamak.

## 2.1   Geometry Definition

As it has been said before, the model has been based in the VEST cylindrical tokamak (Figure 9) [2]. It is a Korean tokamak which geometry is defined by a 3 different sections chamber.
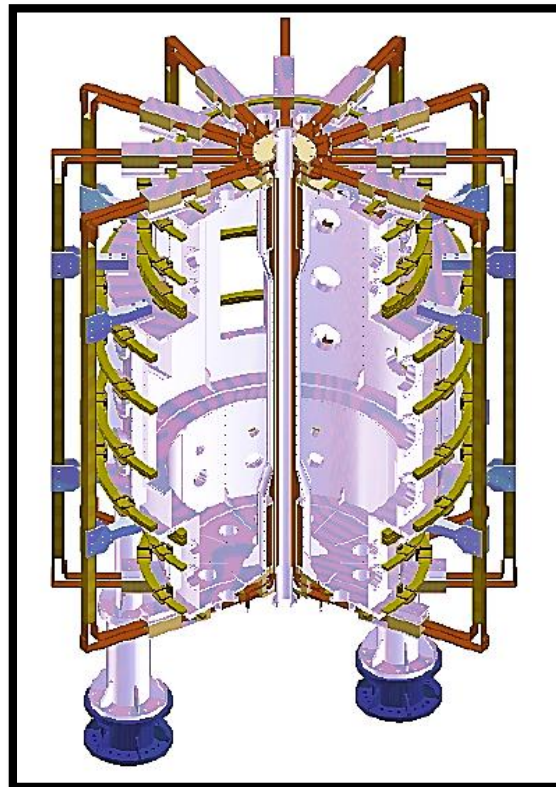


*Figure 9 – VEST*

There are several coils disposed in toroidal and poloidal directions, and, taking advantage of the reduction of the diameter in the upper and lower part of the vacuum vessel, not all the poloidal coils have the same diameter, as shown in Figure 10:
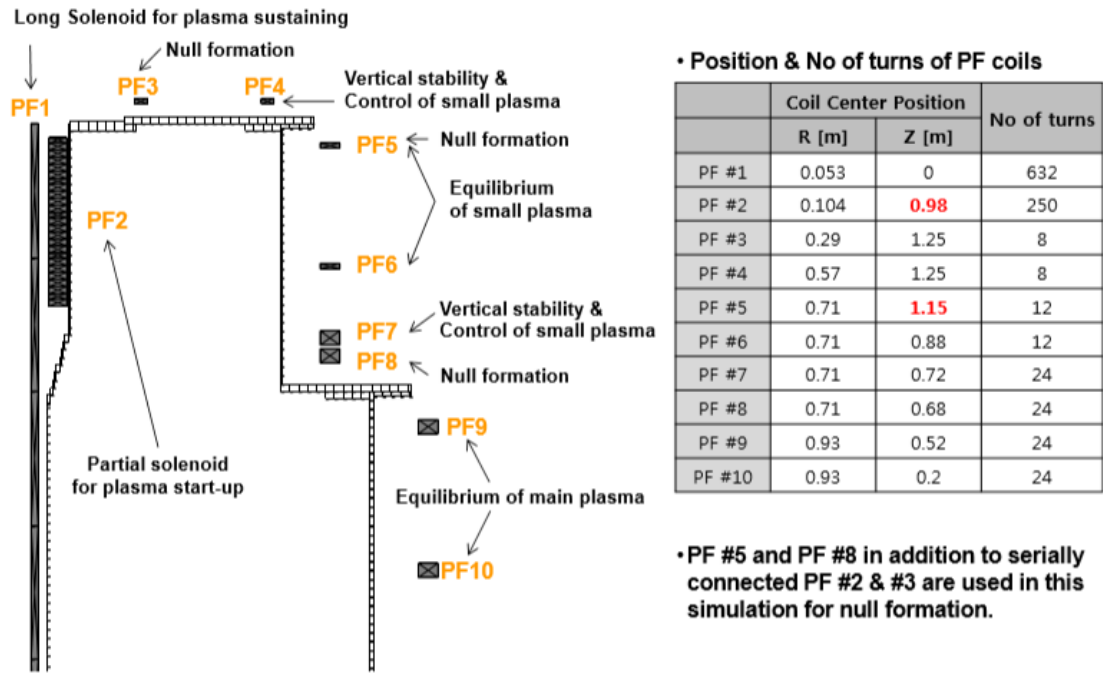
Figure 10 - VEST Tokamak: Coils geometry and location

The tokamak analysed in this project is currently being designed and will have a cylindrical vacuum vessel with constant diameter and 12 coils, distributed as 4 poloidal coils and 8 toroidal coils symmetrically disposed. Some ideas of design of what we want to be the final tokamak are shown in Figure 11 with some details in Figure 12 and Figure 13:
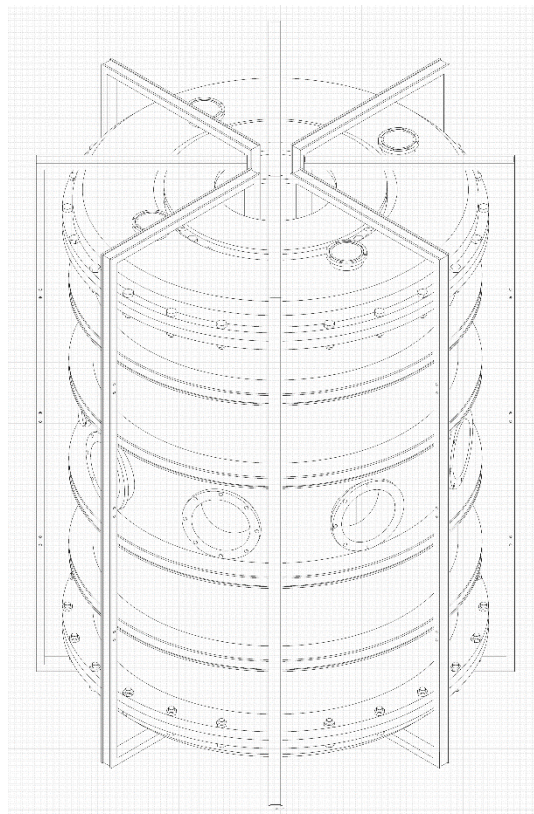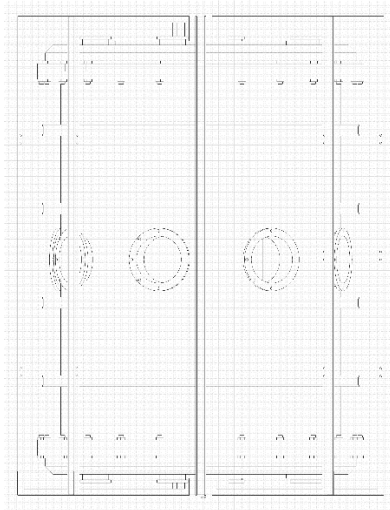


Figure 11 - Tokamak Isometric View
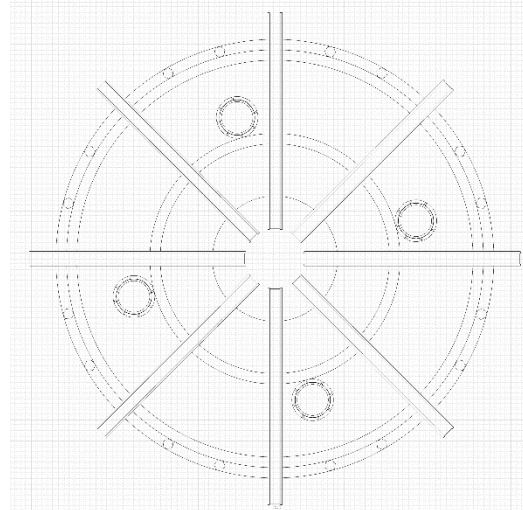
*Figure 12 - Tokamak Front View*



*Figure 13 - Tokamak Upper View*

The coils consist of some coiled wires in a U-profile rails (see Figure 14). This shape of the rails is to restrict the movement of the coiled wires in three of the four possible directions. To restrict the free side, the wires will be attached to the rails with clamps distributed along them.
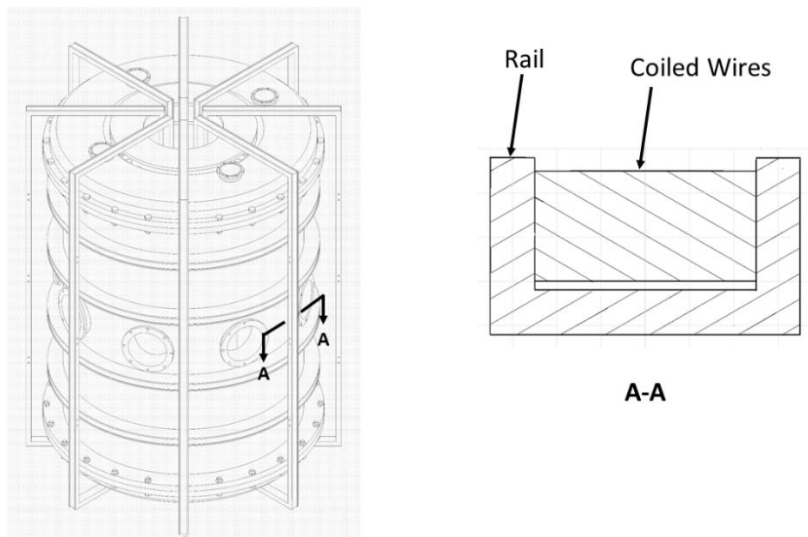


*Figure 14 - U-profile Rails*

For this project, the wires have not been considered from the structural point of view, and the joint of them to the rails has been considered as unbreakable and that transmit all the forces and movements perfectly.

The software CATIA has been selected to develop the CAD model of the Tokamak (see Figure 15). The final assembly is composed on different elements, indicated in Figure 15 that will be briefly described below:

- Vacuum vessel
- Two covers
- 8 Toroidal coils and their rails
- 4 Poloidal coils and their rails
- 96 Supports for the toroidal rails
- U-Structure to fix the supports
- All the fasteners related.

11

The material selected for all the elements is non-magnetic stainless steel (AISI 316L), in accordance with other models of tokamak now in servicing. Apart from low magnetic permeability, this material has the mechanical characteristics needed to support all the forces that the tokamak will generate and receive in the structure.



*Figure 15 - Tokamak Assembly*
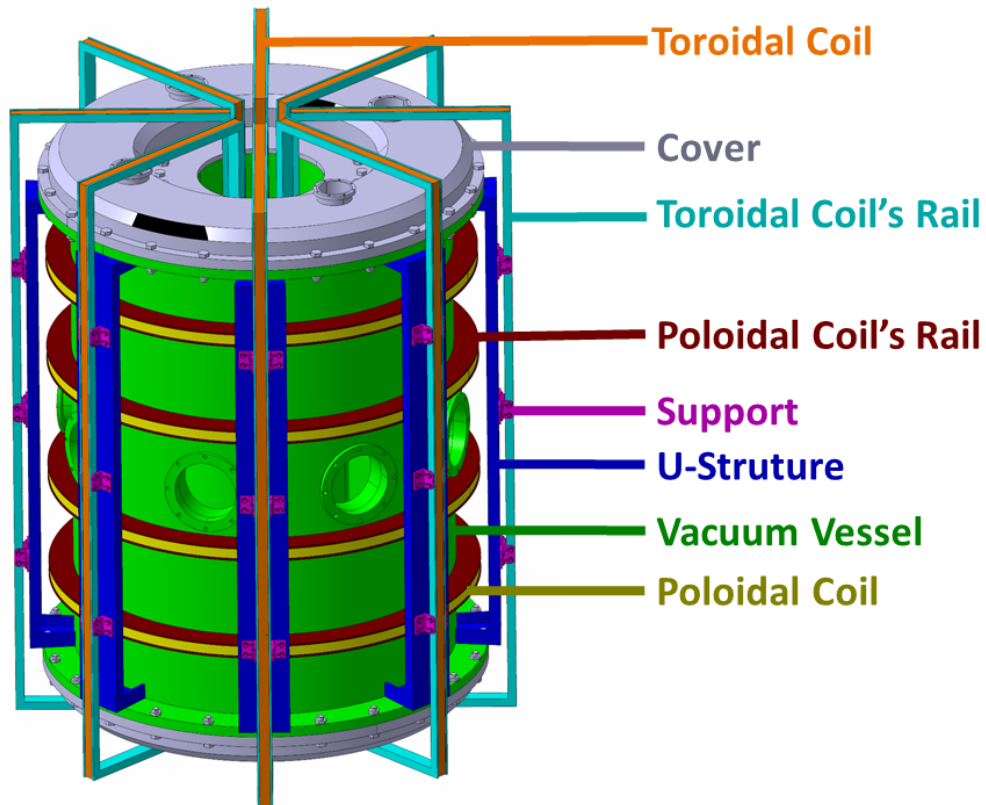
### 2.1.1  Vacuum vessel

The vacuum vessel is the chamber where the plasma is confined. It provides a high-vacuum environment for the plasma, improves radiation shielding and plasma stability and acts as the primary confinement barrier for radioactivity. Due to this high-vacuum environment, the plasma particles spiral around continuously inside the vacuum vessel without touching the walls, which avoid the heat transfer by convection from the plasma to the walls. To remove the rest of the heat generated during the operation, there is cooling water that circulates through the vessel's steel walls.

In this case, as shown in Figure 16, is the space between two concentrically cylinders of radius 0.4 m and 0.8 m. On the tips of the lateral sides, a surface has been generated to attach the covers on it with the help of some bolts distributed circularly along the internal and external radius. It is inspired on the vacuum vessel design of the VEST tokamak.

Furthermore, 8 ports have been installed on the lateral side of the vacuum vessel in a similar disposition that in the ST25D tokamak, developed by Tokamak Energy (UK) (see Figure 16). They provide access for remote handling operations, diagnostics, heating, and vacuum systems.
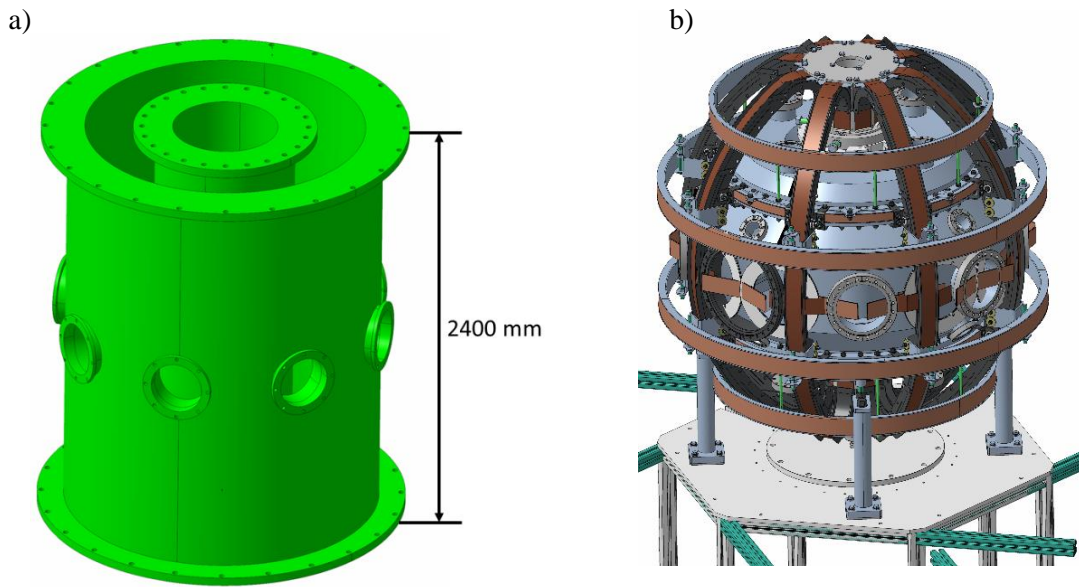
*Figure 16 – a) Vacuum Vessel  b) ST25 Tokamak (Tokamak Energy, UK)*

## 2.1.2  Covers

They are installed on both extremes of the vacuum vessel and his main function is to close the vacuum vessel to allow the vacuum generation. Both upper and lower covers have an identical design with an external diameter of 2.1 m and have 4 ports installed (see Figure 17):
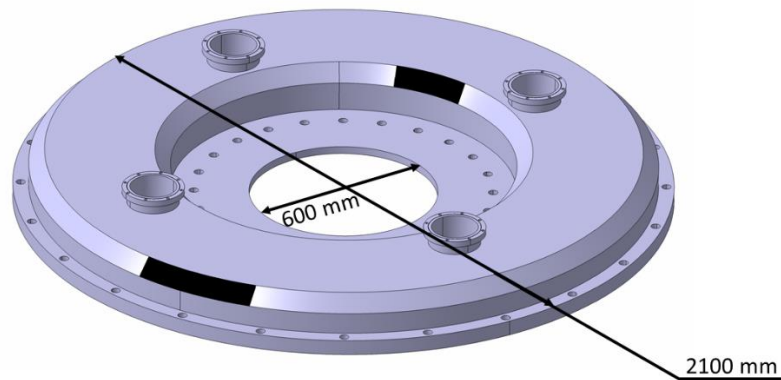


*Figure 17 - Cover*

## 2.1.3  U-Structure

The U-structure fulfils a structural objective and is to provide to the coils supports a place where they can be fixed. The U-structure is attached to the vacuum vessel using the same joint/fasteners than the covers. Its geometry is shown in Figure 18:
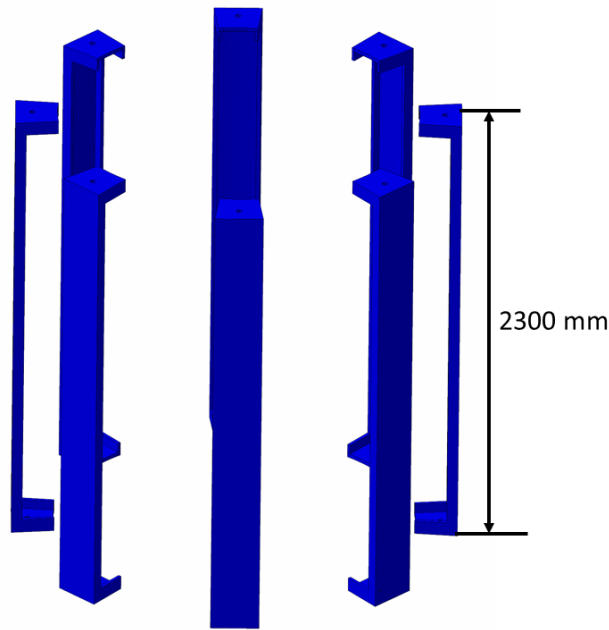
*Figure 18 - U-Structure*

## 2.1.4    Toroidal coils

The toroidal coils have a rectangular shape with dimensions of 3 m x 1 m (see Figure 19). The number of loops of the wires around the rails will depend of the final design of the tokamak power supply. Their design is conditioned by the electrical current that flows through the coil and the way it will be controlled. The internal part of them will be located within the central column of the tokamak.

The toroidal coils are attached to the tokamak with the supports described later, and being their design the objective of this project.
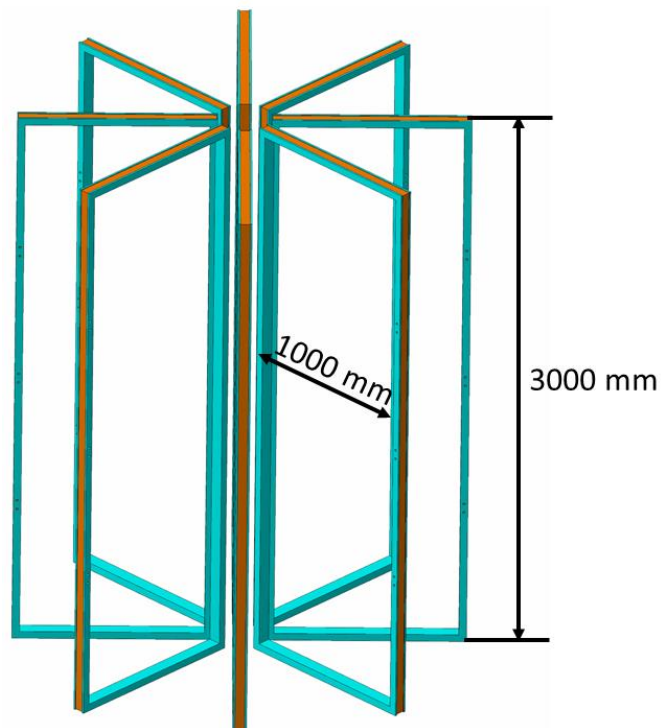


*Figure 19 - Toroidal Coils and Rails*

## 2.1.5   Poloidal coils

The poloidal coils have a circular shape of 2 m of diameter (see Figure 20). Each of them consists of a long wire that round the rail. As for the toroidal coils, the number of loops of the wires around the rails will depend of the final design of the power supply of the tokamak. The rails have been designed in a way that they will be welded to the vacuum vessel.
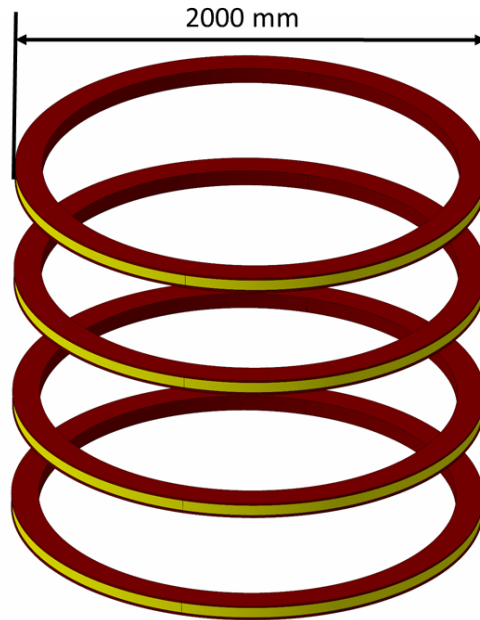


*Figure 20 - Poloidal Coils and Rails*

## 2.1.6   Supports

Their design is the objective of the project. They are used to attach the rails of the toroidal coils to the U-structure. They must be able to resist the stress generated on them as a consequence of load transferred by the toroidal field coils. Their final design is shown in Figure 21:
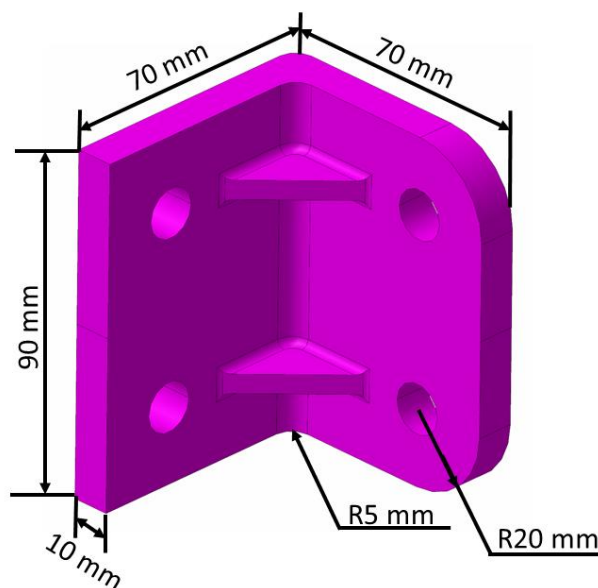


*Figure 21 - Support*

## 2.1.7 Assembly

Finally, the assembly with all the parts installed is shown in Figure 22. Some constructive details can be found in Figure 23, Figure 24, Figure 25 and Figure 26:



*Figure 22 - Tokamak*
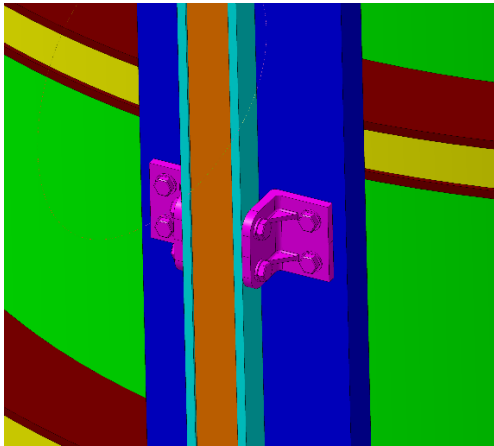
*Figure 23 - Supports Installed*
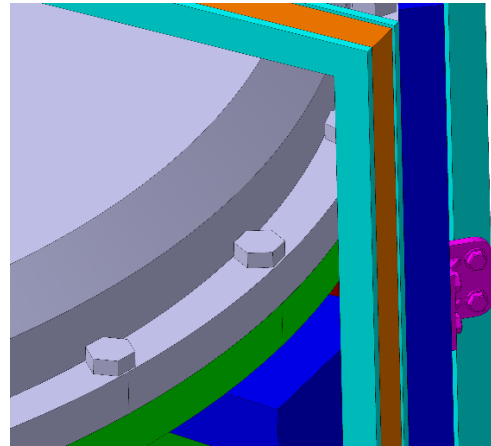

*Figure 24 – Fasteners*
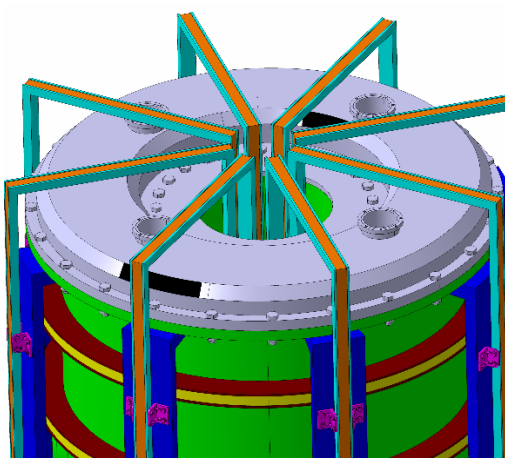

*Figure 25 - Cover Installed*
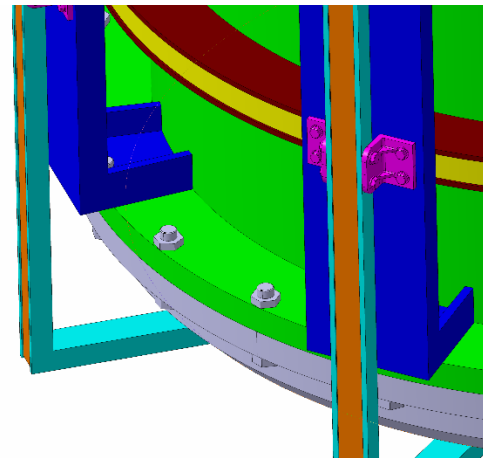

*Figure 26 - U-structure Installed*

## 2.2   Electrical Configuration

As explained in the Tokamak section, it is a device that works inside a magnetic field generated by the toroidal and poloidal coils. Through them flow some electrical currents of very high intensities. This magnetic field provokes some stress in the coils that must be withstand by the structure in order to allow to the tokamak to continue its operation. Therefore, in order to calculate the stresses (and design the supports), it is necessary to know the electrical current delivered to every coil.
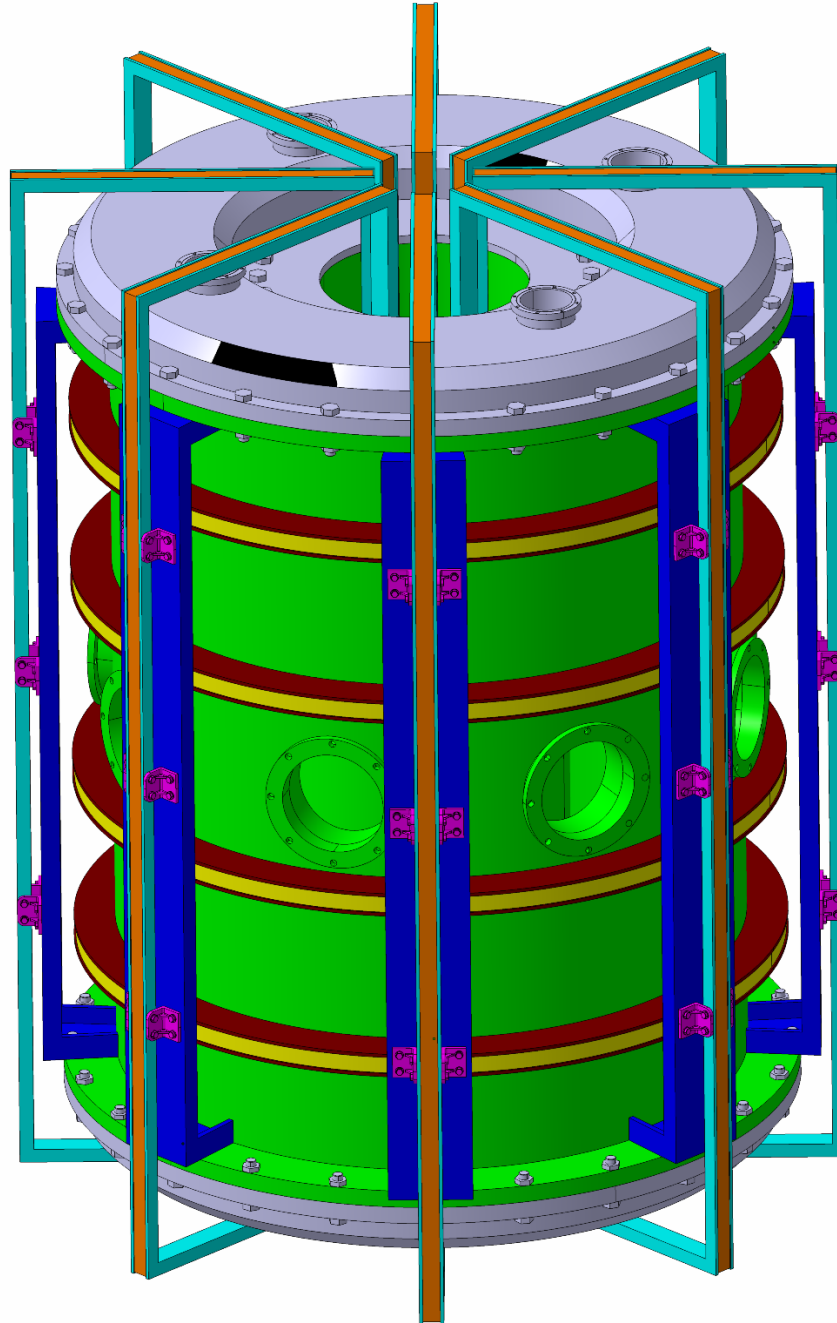
In this section, the electrical configuration for the tokamak is explained and, for that, the currents flowing along the coils are described. The choice for the sign of the current in the coils is:

- For the toroidal coils, in the lid inside the tokamak column, the flow must go from the bottom to the top, as shown in Figure 27. The intensity will be the same for all of them.
- For the poloidal coils, the currents flow in different directions, clockwise and anticlockwise direction, as shown in Figure 28 and Figure 29, and do not need to have the same intensity.

As for the geometry, the values of the intensity have been inspired in the VEST model (Figure 9). Following this origin and the restrictions set before:

- **Toroidal coils:** The currents flow with an intensity of 75000 A in all the coils , as shown in Figure 27
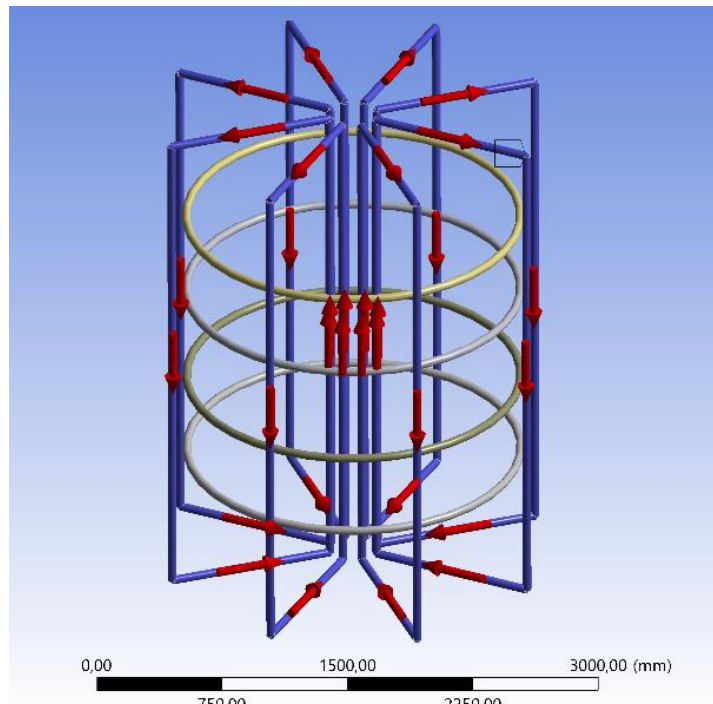


*Figure 27 - Poloidal Coils Electrical Configuration*

- **Upper and lower coils:** The currents flow with an intensity of 40000 A in anti-clockwise direction looking from top in the upper and lower coils, as shown in Figure 27.
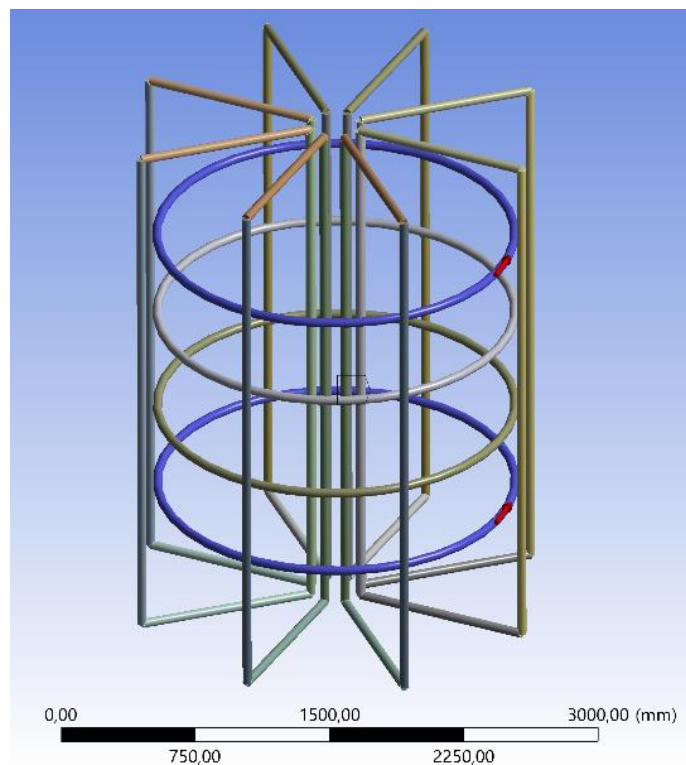


*Figure 28 – Top and Bottom Toroidal Coils Electrical Configuration*

- **Middle coils:** The currents flow with an intensity of 15000 A in clockwise direction looking from top in the middle coils, as shown in Figure 29.
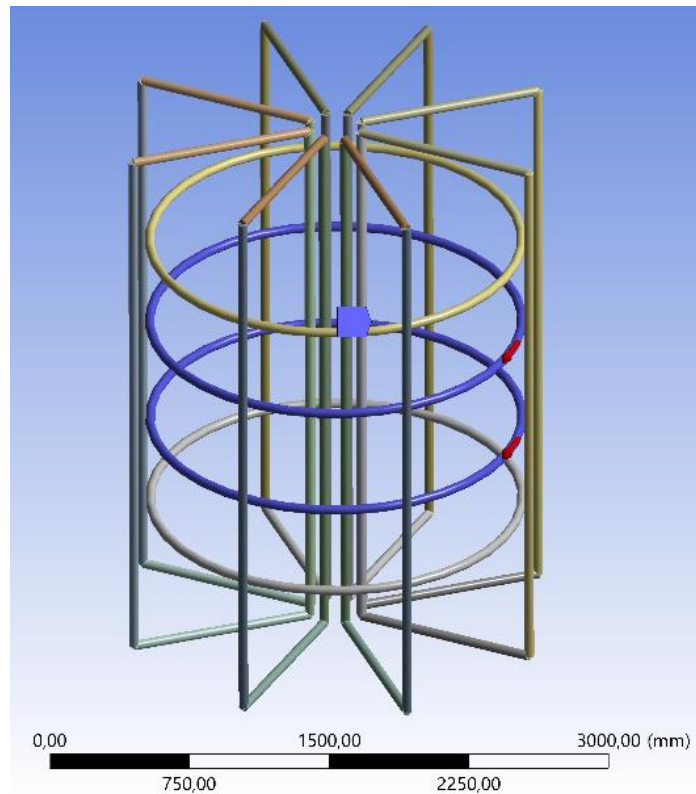


*Figure 29 - Middle Poloidal Coils Electrical Configuration*

## 2.3   Theoretical Background

As stated before, for the Tokamak operation, a magnetic field will be generated by energizing different sets of coils. The current flowing through the coils, in presence of this magnetic field will induce forces in the wires that will be transferred to the rails and, therefore, to the supports. Two physical Laws can be used to describe these phaenomena:

- Biot-Savart law
- Lorentz force law

We start from the initial idea that we have some coils that will be energized by an electric current. The Biot-Savart law explains that these electrical currents will generate a relevant magnetic field in the work area of the tokamak. Complementing this information, the Lorentz force law explains that if we have a coil with current inside of a magnetic field, a force will be induced in the coil called Lorentz force. If only one coil would exist in the model, this magnetic field does not generate a problem for us, since the coil will be in equilibrium. However, we have several coils of different geometries and in different position that will generate and receive forces generated by the currents that flows from the other ones.

A detailed description of these laws is given below.

## 2.3.1 Biot-Savart law

The Biot Savart Law [3] is an equation that describes the magnetic field generated by a constant electric current. It relates the magnetic field to the magnitude, direction, length, and proximity of the electric current.

This law is fundamental to magnetostatics, playing a role similar to that of Coulomb's law in electrostatics.

The Biot Savart law was developed by two French physicists, Jean Baptiste Biot and Felix Savart derived the mathematical expression for magnetic flux density at a point due a nearby current carrying conductor, in 1820. Viewing the deflection of a magnetic compass needle, these two scientists concluded that any current element projects a magnetic field into the space around it.

Through observations and calculations, they had derived a mathematical expression:

$$B = \frac{\mu_0 * I}{4 * \pi} \int \frac{d\vec{r}' * (\vec{r} - \vec{r}')}{|\vec{r} - \vec{r}'|}$$

This is the vectorial equation of the law, to simplify this, and illustrate itself we are going to show an example in Figure 30:
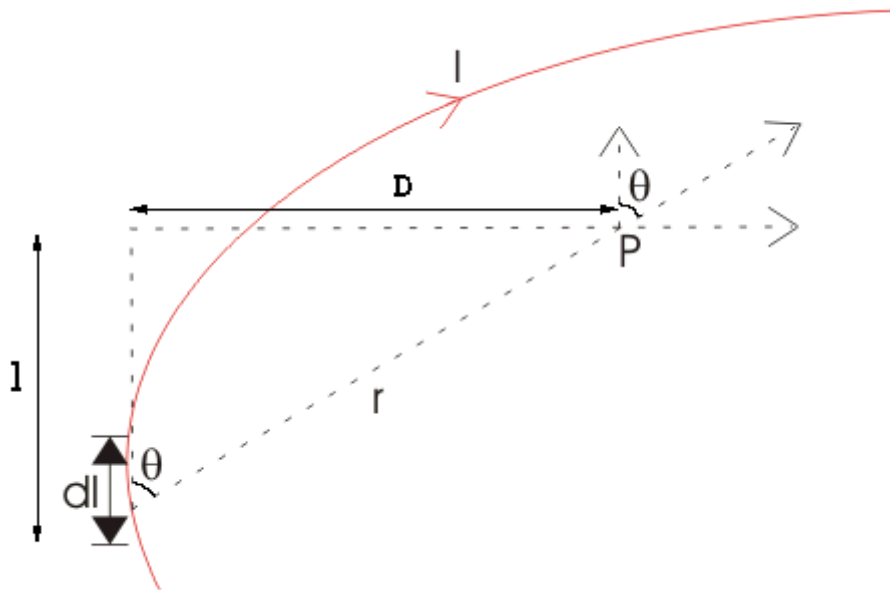


*Figure 30 - Biot-Savart law*

It shows an infinitesimal application, where the magnetic flux density of dB, is directly proportional to the length of the element dl, the current I, the sine of the angle and θ between direction of the current and the vector joining a given point of the field and the current element and is inversely proportional to the square of the distance of the given point from the current element, r

$$dB = k * \frac{I * dl * \sin \theta}{r^2}$$

Where:

$$k = \frac{\mu_0}{4 * \pi}$$

$\mu_0 \rightarrow$ absolute permeability of the environment, for the air $\mu_0 = 4 * \pi * 10^{-7} \, W_b/A - m$

And the final equation will be:

$$dB = \frac{\mu_0}{4 * \pi} * \frac{I * dl * \sin\theta}{r^2}$$

### 2.3.2 Lorentz force law

The Lorentz force is the force exerted on a charged particle $q$ that moves with a velocity $\vec{v}$ through an electric field $\vec{E}$ and magnetic field $\vec{B}$. The whole electromagnetic force (Lorentz force) $\vec{F}$ is calculated:

$$\vec{F} = q * \vec{E} + q * \vec{v} \times \vec{B}$$

Where the first term is the contribution of the electric field and the second one is the magnetic force, which has a direction perpendicular to the current direction and the magnetic field. For magnetism issues, the component of the force due to the electrical field is usually discard:

$$\vec{F} = q * \vec{v} \times \vec{B}$$

If there is an angle $\phi$ between $\vec{v}$ and $\vec{B}$, the magnitude of the force is:

$$F = q * v * B * \sin\phi$$

There are some interesting situations depending on the value of $\phi$:

- If $\phi = 90°$ the particle will follow a circular trajectory with a radius $r = mv/qB$
- If $\phi < 90°$ the particle orbit will be a helix with an axis parallel to the field lines
- If $\phi = 0°$ there will not be magnetic force applied on the particle, which will move undeflected along the field lines.

If we want to see the integral equation of the law:

$$F = I * \int_a^b \vec{u_t} \times \vec{B} * dl$$

Where:

$$I \rightarrow \text{intensity of the current}$$

$$\vec{u_t} \rightarrow \text{direction vector of the current}$$

$$\vec{B} \rightarrow \text{magnetic field vector}$$

$$a \text{ and } b \rightarrow \text{points that defines the geometry of the segment}$$

The magnetic force on a moving charge shows the sign of the charge carriers in a conductor. A current that flows from the right to the left in a conductor can be the result of a positive charges carrier moving from right to left or a negative charges moving from left to right (or a combination of them). If the conductor is placed in a magnetic field perpendicular to the current, the magnetic force on both types of charge carriers will be in the same direction. This force provokes ta small potential difference between the sides of the conductor. This is known as the Hall effect. This effect occurs when an electric field is aligned with the direction of the magnetic force.

If a wire with a current $I$ is placed in a magnetic field $B$, how we can calculate the force on the wire? As a current represents the movement of some charges along the wire, the Lorentz force is applied on the moving charges. As these charges are bound to the conductor, the magnetic forces on the moving charges are transferred to the wire. The force on a small length $dl$ of the wire depends on the orientation of the wire with respect to the field. The magnitude of the force is:

$$dF = I * dl * B * \sin \phi$$

If $\phi = 0$ or $180°$, there will be no force. That means that the current is parallel to the field direction. On the other hand, the maximum force will be obtained when the current and the field are perpendicular to each other $\phi = 90°$. In that case:

$$dF = I * dl * B$$

## 2.4  Solution Workflow

In this section, the approach used for solving the design problem of the supports for the toroidal field coils of a tokamak is briefly described.

Once the basic tokamak design parameters have been described, the procedure developed for designing the supports will be explained. For this, the initial idea was to simulate the whole model in the software ANSYS, and obtain the magnetic field value as the first solution, and use this data to obtain the forces generated on the supports. However, due to the lack of knowledge with the free (and available) magnetism module of ANSYS, it was decided to solve simple problems with ANSYS and compare the results with the theoretical ones.

With this check, we discovered that the forces calculated due to a magnetic field were out of the range of chances for the values of the current intensities. So, it was decided that the work was going to be done in two different ways in parallel.

The first one, has been the simulation of the tokamak theoretically with Matlab, and the other one, using a Finite Element Method (FEM) with the software ANSYS. The idea of this duplicity was to make sure that the results were correct before start with more important issues.

When the forces were calculated, the supports were designed in order to fit the structural requirements of the problem.

The flowchart given in Figure 31 shows schematically all the steps given during the development of the work:

# Magnetic Field Calculation

Numerical methodology (FEM ANSYS)

↓

Generation of coils' geometry

↓

Resolution of easy magnetic field problems

↓

Calculation of magnetic field generated by coils

Analytic methodology (MATLAB)

↓

Generation of tokamak's geometry

↓

Calculation of magnetic field generated by tokamak

MATCH?

# Force Calculation

Calculation of forces in MATLAB

↓

Design and generation of supports geometry in ANSYS
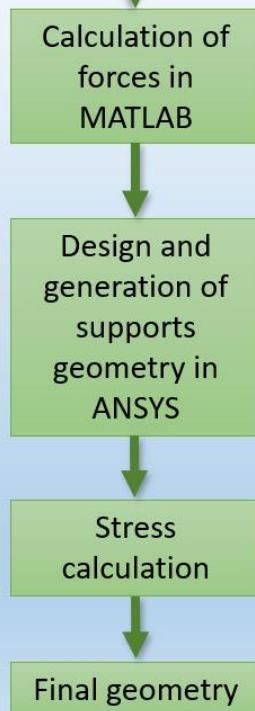
↓

Stress calculation

↓

Final geometry

*Figure 31 - Flowchart*

# 3 Assessment of the coils supports

## 3.1  Magnetic Field Estimation

The first step of the solution process is to calculate the magnetic field generated by the coils of the tokamak. As explained above, due to the Biot-Savart and Lorentz force laws, the electrical currents flowing through the coils will generate a very intense magnetic field into which the tokamak is immersed. Then, this magnetic field will cause the forces that we have to calculate to assess the coils supports.

Therefore, we have to try to simulate the electrical problem as accurately as possible, and this will be the objective of this section. To do this, and in order to avoid some importation/exportation problems and to assure the proper performance of the model, we decided to create the geometry of the coils with the design modeller of ANSYS Workbench.

From the point of view of the magnetostatic study, we only need the design of the coils. Therefore, it was decided to keep the rest of the tokamak structure without modelling it (see Figure 32). If we analyze the Figure 32, we can see that the coils have been modelled as cylinders. It may give the impression that is single large wire, but, obviously, this is not real. Perhaps, from a design point of view, the most accurate way to draw the coils would be a rectangle that represent all the turns that the wire will have around the rail. However, it was verified with the resolution of some theoretical examples (not attached in this document) that the most reliable configuration was the cylindrical representation.



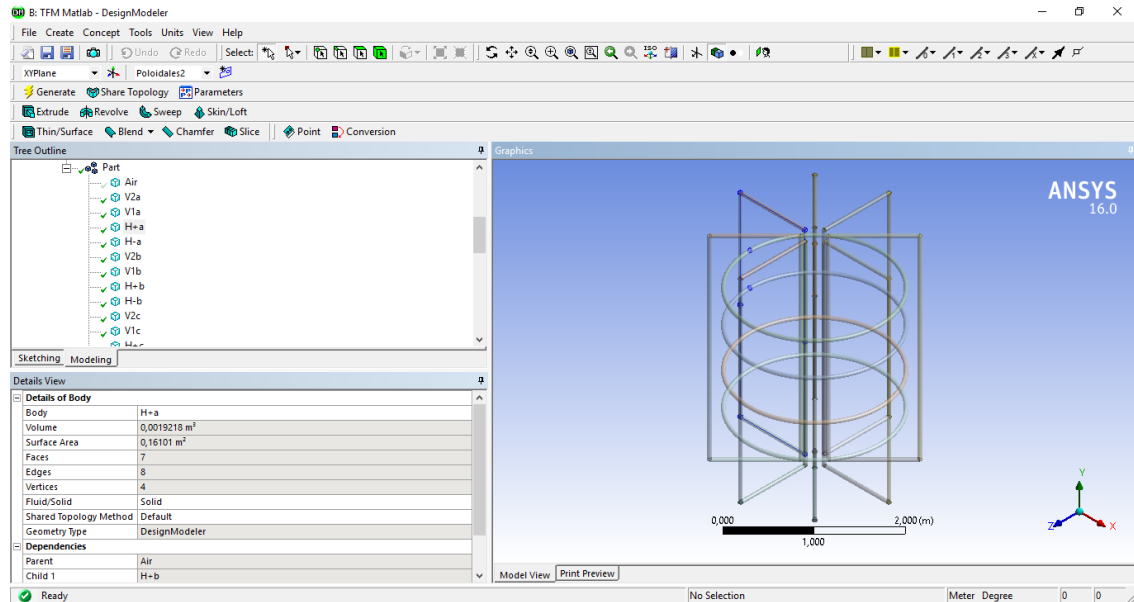*Figure 32 - Tokamak Magnetostatic Analysis*

Both types of coils have been designed with different configurations. On the one hand, the toroidal coils are divided in 4 different bodies (2 horizontals and 2 vertical wires/cylinders). On the other hand, each poloidal coil has been created as a one continuous body. The differences between them, and the cause to divide the rectangular coils in 4 segments are:

- The calculation of the magnetic field in ANSYS for segments is really excellent and with a higher level of precision than for closed bodies (that does not mean that is bad for them, only less approximate). One of the main reasons of this is that when adding a current that flows through a body, it is automatically set in the direction of the Y-axis associated with the body. In the case of the 4-segments problem, each segment has its own coordinate system associated and there is no problem with this, but, for a rectangle, we only have one body (and we can only associate one coordinate system). In this case, it is necessary to work as in the problem of the circular coil, and create a cylindrical coordinate system that does not work as well as in a circular coil resolution.

- In addition, the computational limit is another important cause. In order to have a mesh which can work on this tokamak and solve the model with a minimum of requirements, we are not going to have it as refined as we would like on the coil, which causes that the continuity of the mesh in the corners of the rectangle is not as ideal as needed.

Since the magnetic field generated by a closed rectangular coil is the vectorial sum of the magnetic fields generated by the segments that compose it, we can apply this alternative and continue obtaining the expected result with the necessary precision [4].

It is obvious that from the point of view of working in the design module, it seems to be less productive to design 4 separate segments with their own coordinates system than designing a single rectangle, but this makes (as explained above) more precise the resolution of the problem using the magnetostatic module.

As the bibliography about this module is not too complete, it is necessary to check which is the correct way to set the module on our own. In order to do this, a benchmarking has been done, testing different models and configuration and comparing the results with the theoretical ones. These exercises are composed by the analysis of 1 rectangle coil (similar to the toroidal coils) and 1 circular coil (similar to the poloidal coils).

### 3.1.1 Examples: Magnetic field due to current carrying elements

#### 3.1.1.1 Rectangular coil

As explained above, for a closed rectangular coil, the magnetic field generated by a current that flows through it can be calculated as the sum of the magnetic field generated by each segment of the rectangle.

To measure the accuracy of the ANSYS software to the theoretical problem, the Problem 1 has been solved. This problem was solved with the two ways explained before, with the rectangle coil as a single whole body, or as 4 segments joined at the tips. Experience has shown that the 4-segments method presents more accurate results compared to the theoretical ones, so only this one will be shown here:

##### 3.1.1.1.1 Problem 1

For a rectangle coil with side measures of $a = 3\ m$ and $b = 10\ m$, in which flows a current with an intensity of $I = 100\ A$ (see Figure 33).

1. Calculate the magnetic field (B) on an imaginary line on the plane of the coil that go through the centroid of the coil and compare the result with the theoretical one.
2. Calculate the magnetic field (B) on an imaginary line on the plane of the coil that go through the 75% of b from the centroid of the coil and compare the result with the theoretical one.

3. Calculate the magnetic field (B on an imaginary line on the plane of the coil that go through the 90% of b from the centroid of the coil and compare the result with the theoretical one.
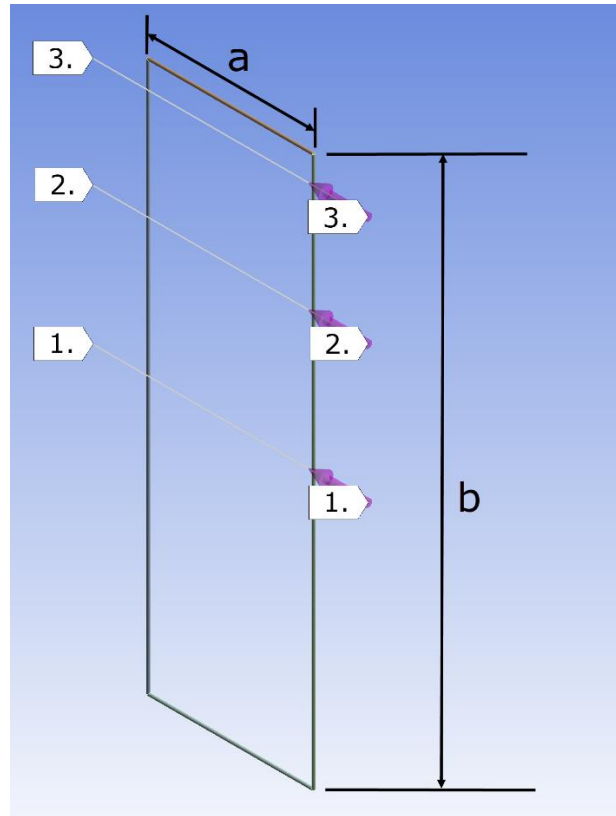


*Figure 33 - Problem 1*

### 3.1.1.1.1.1 Solution P1

To calculate the theoretical results of the magnetic field we have to apply de Biot-Savart law:

$$dB = \frac{\mu_0}{4 * \pi} * \frac{I * dl * \sin \theta}{r^2}$$

After the theoretical calculation through the lines selected in the 3 statements of the problem and taking them as reference, both the theoretical results and FEM (ANSYS) are represented in the graphs in the Figure 34 (50% of b), Figure 35 (75% of b) and Figure 36 (90% of b):
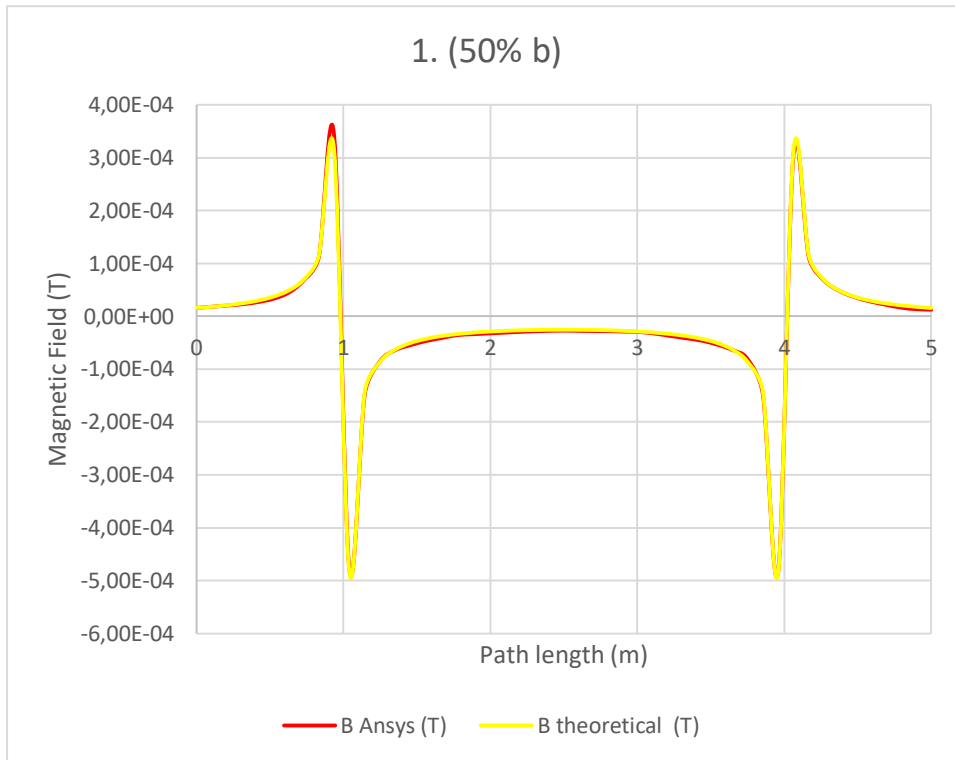
*Figure 34 - Problem 1 - Solution 1. At 50% b*

As can be seen in Figure 34, both results are very similar, practically the same. In order to see the real accuracy of ANSYS, we have calculated the mean error percentage between the theoretical value and the ANSYS value and it is 5.7 %.

For the questions 2. and 3. similar results are obtained in Figure 35 and Figure 36 respectively:
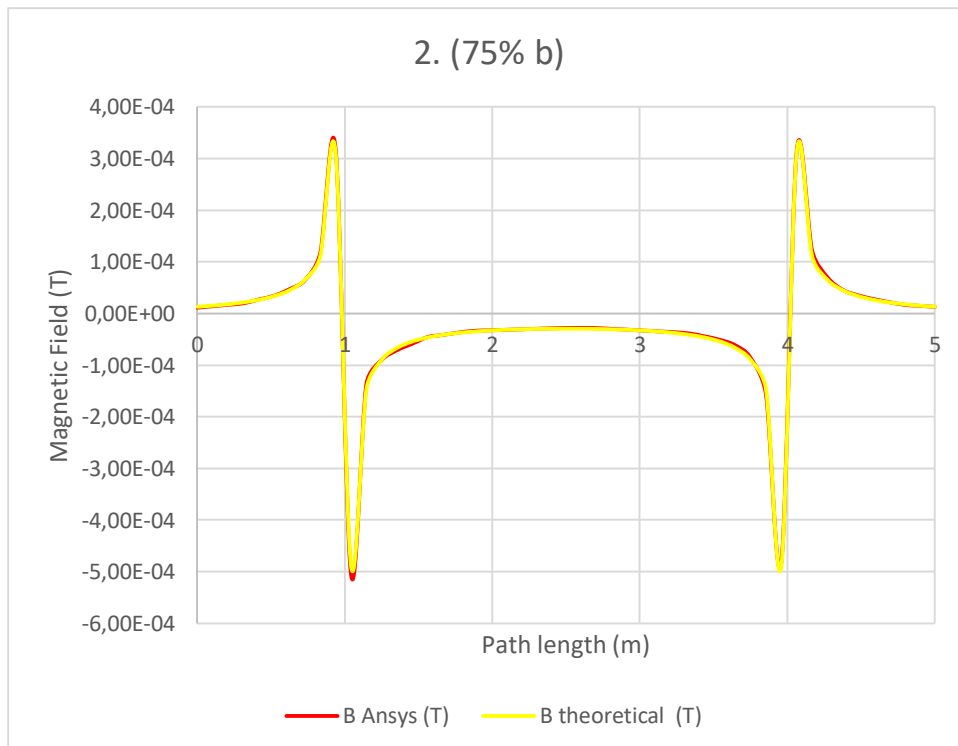


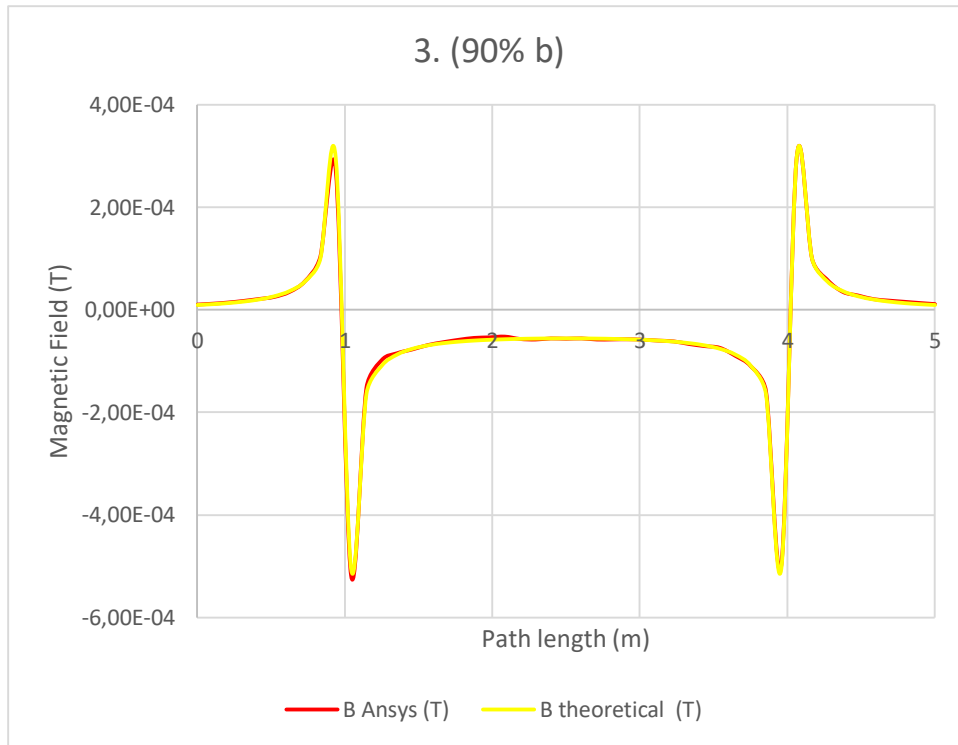*Figure 35 - Problem 1 - Solution 2. At 75% b*

*Figure 36 - Problem 1 - Solution 3. At 90% b*

Calculating the exact mean error percentage between the theoretical value and the ANSYS one, it is set at 4% for the second case (75% of b) and 4.2% for the third (90% of b).

As it has been calculated, the biggest error of the three cases is less than 6%. We think that the average error is close enough to zero, and we consider acceptable the results from ANSYS for the rectangle coils, which give us the option of simulating the toroidal coils with acceptable accuracy.

### 3.1.1.2    Circular coil

For this case, we are going to simulate a circular coil and compare the generated results with the theoretical ones.

To measure the accuracy of the ANSYS software to the theoretical problem, the Problem 2 has been solved:

#### 3.1.1.2.1    Problem 2

For a circular coil with a radius measure of $r = 1\,m$ in which flows a current with an intensity of $I = 800\,A$.

1.  Calculate the magnetic field (B) on the axis of the coils on a length from its plane to 5 meters away of it and compare the result with the theoretical one.

#### 3.1.1.2.1.1    Solution P2

First, to obtain the theoretical results, it is necessary to adapt the formula of the Biot-Savart law to calculate the magnetic field (B) applied to a point on the axis of a circular coil:

$$B = \frac{\mu_0 * I * r^2}{2 * \left(\sqrt{z^2 + r^2}\right)^3}$$

28

Where r is the radius of the coil, I the intensity of the current and z the distance from the point to the plane of the coil.

For the value of the magnetic field on the centroid of the coil (z=0):

$$B = \frac{\mu_0 * I}{2 * r}$$

Now that we have the theoretical expression, we have to obtain the magnetic field from the simulation in Ansys. For this, the tool "path" of the electromagnetic module has been used to show the results, as in the Problem 1 (see Figure 37):
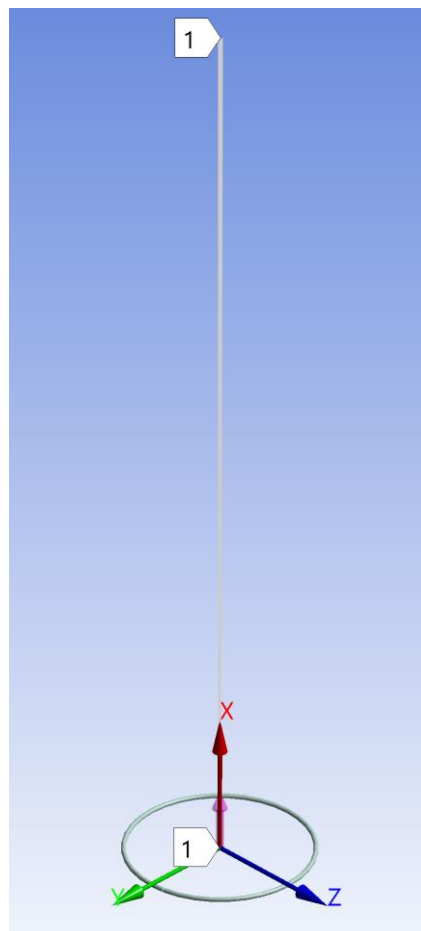


*Figure 37 - Problem 2*

For the circular coils, as explained before, it is necessary to generate a cylindrical coordinate system associated to them in order to establish the direction of the current of the system.
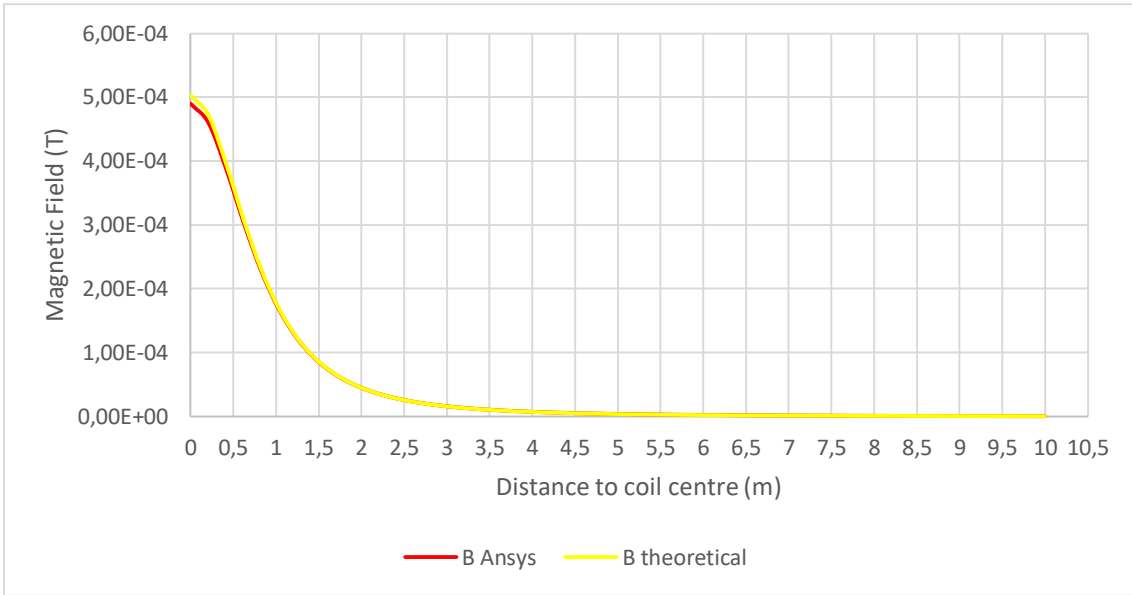
If we compare both results:

*Figure 38 - Problem 2 - Magnetic Field*

As it is visible in Figure 38, both results are very similar, they do not match as in the Problem 1, but a real accuracy between them is shown. In order to see the actual accuracy of ANSYS, we have calculated and represented the error percentage between the theoretical value and the ANSYS value in the Figure 39:
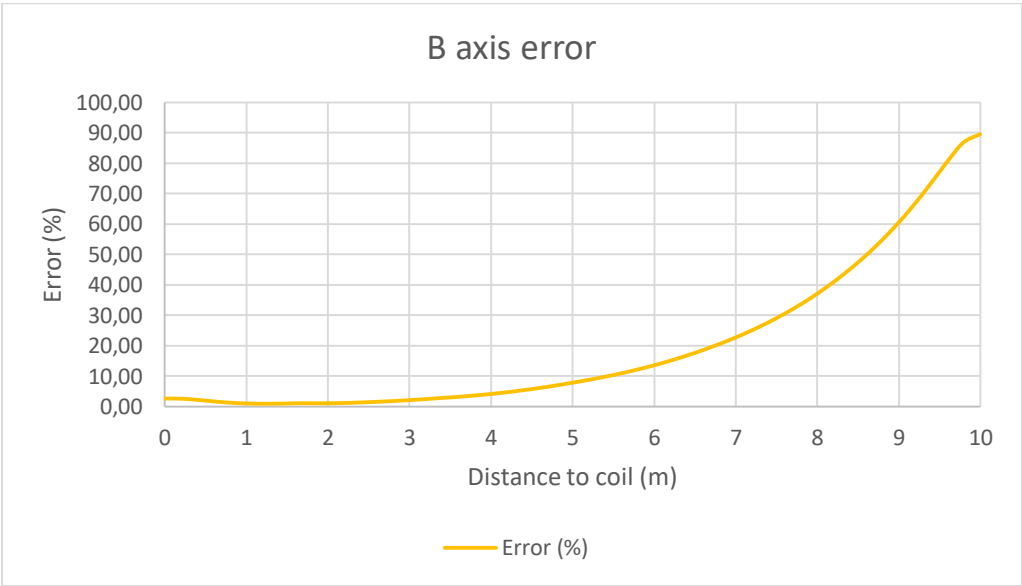


*Figure 39 - Problem 2 – Error %*

This graph (Figure 39) may introduce the idea that the error is not acceptable (about 20 % on average), and, if we only take the number, we should discard this method, but, by studying the numbers more specifically, and analysing the results area by area, we can obtain different conclusions. Specifically, if we extract the first 4 meters from the coil through the axis, as represented in Figure 40:
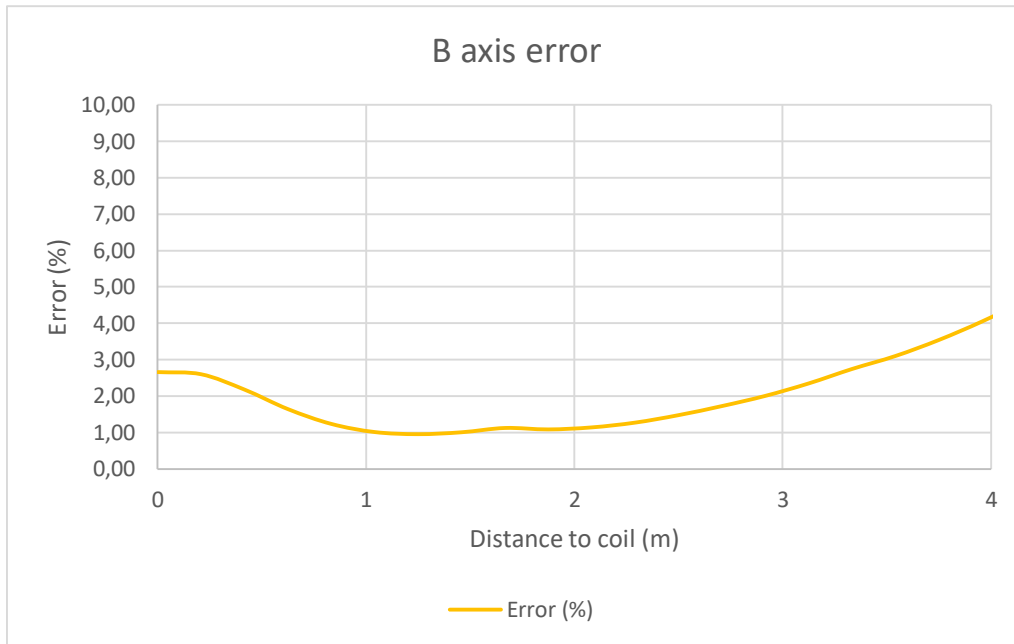
*Figure 40 - Problem 2 – Error % (0 to 4 meters)*

They are very similar, practically the same. Taking the numbers, the mean error is 1,95 %. The main problem (as in the Problem 1) for the high error value away from the coil is that the values of the magnetic field are very low ($10^{-6}, 10^{-7}$), so a small variation in the results generates very high error percentages.

Obviously, as the error value in the main calculation area is very close to 0%, we consider that the simulation in Ansys is acceptable and we can use the extrapolation and the mixing of both methods (rectangular and circular coils) for our model.

### 3.1.2 Tokamak model

Once we have discovered a successful way to simulate and calculate the magnetic field in ANSYS, it is time to check if this software allows us to know the forces generated on a body by this generated magnetic field.

Some exercises have been done comparing the solution in ANSYS with the theoretical one, but, although the results are always of the same order of magnitude as the theoretical ones, unfortunately, none of them returns values with sufficient precision so that they can be taken into account.

This is a big problem because from the point of view of the resolution of the whole project it would save a lot of time to reach the same solution. But, looking at it from a positive point of view, it will allow us to calculate the forces following the theoretical equations and obtain a better distribution of them along the rails (those that really suffer the efforts, not the wires), which makes us to simulate the forces in a more precise way to obtain the stresses on the supports (explained in Supports assessment section).

In conclusion, we have demonstrated that ANSYS is a useful software to calculate de magnetic field generated by the tokamak, but we will need another way to calculate the forces generated by this magnetic field on the different coils.

This one is the point that leads us to develop the same tokamak in the software Matlab, to obtain the results that we want, and, keep the results from ANSYS as a back-up to confirm them.

Thus, we design the geometry of the coils of the tokamak in ANSYS (Figure 41), and apply all the configuration (mesh size, type, materials, environment…) as in the simple problems extrapolating to the whole model to know the magnetic field generated at all the points of the space:
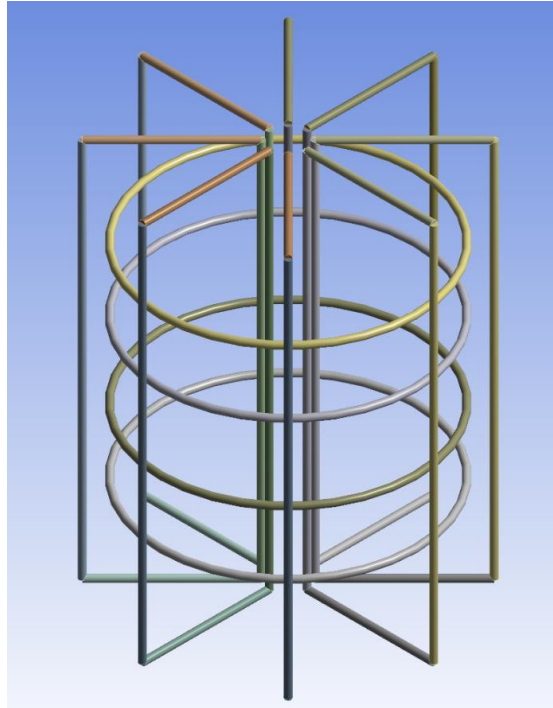


*Figure 41 - Tokamak*

The magnetic results obtained (Figure 42) will be exposed in the

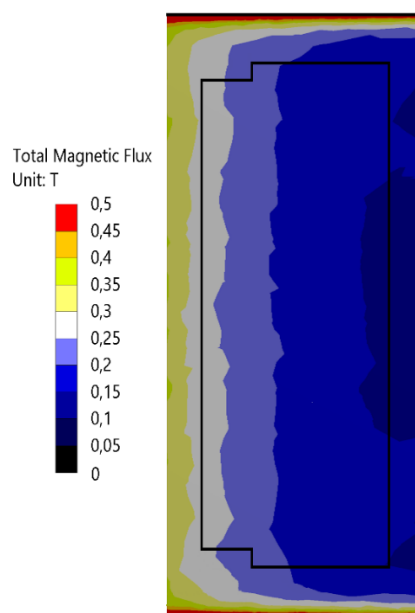Forces estimation section comparing them with the results from Matlab.



*Figure 42 - Magnetic Field Ansys Results*

Now, the problem has been solved by developing a tokamak calculation code [5] and adapting it to our own data. In this code, the magnetic field of each coil will be calculated separately, and then, using the superposition principle, we will be able to sum and obtain the magnetic field configuration.

For the resolution, and with the idea of comparing the results, we are going to obtain the magnetic field in a plane in which one toroidal coil is contained and consider that the problem is fully symmetrical (hypothesis taken from the results in ANSYS), so that the magnetic field will be the same for the whole plane of the coil. The design of the coils of the tokamak is shown in Figure 43:
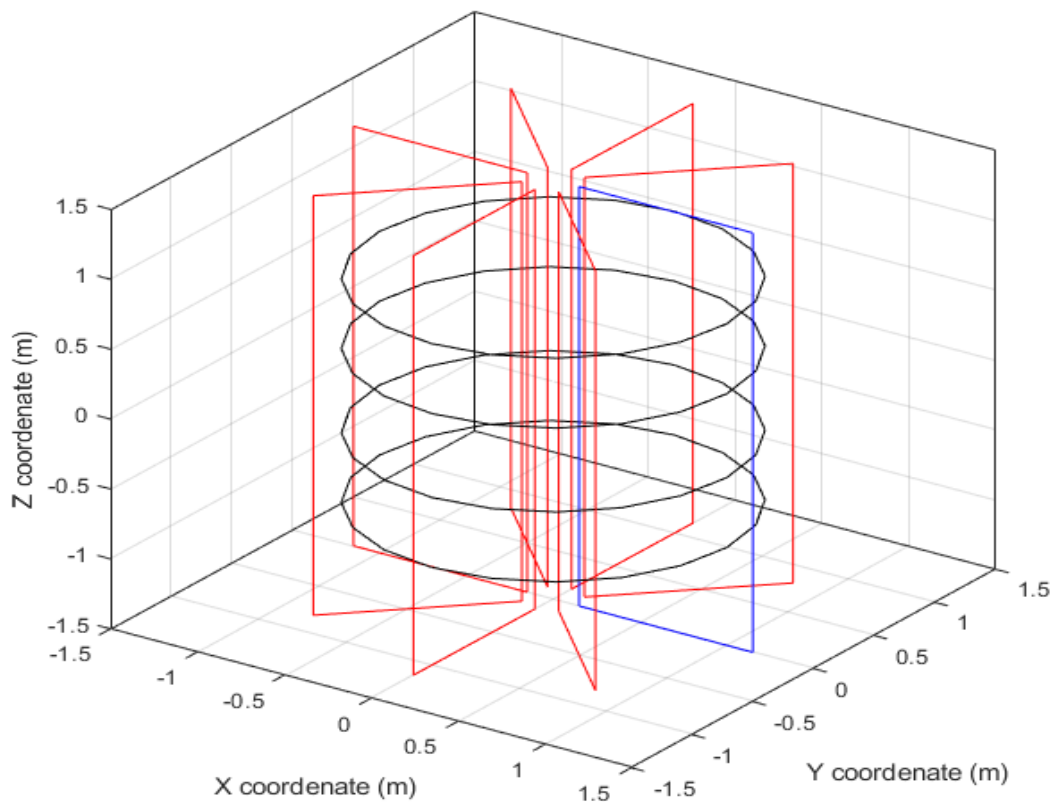


*Figure 43 - Tokamak in Matlab*

Where poloidal coils are black, and toroidal coils are the red and the blue ones, being the plane where we are going to obtain the results, the plane which contains the blue coil.

Then, to make a real comparison between the Matlab (Figure 44) and ANSYS (Figure 45) results, we should do it with the value of the magnetic field inside the vacuum vessel:
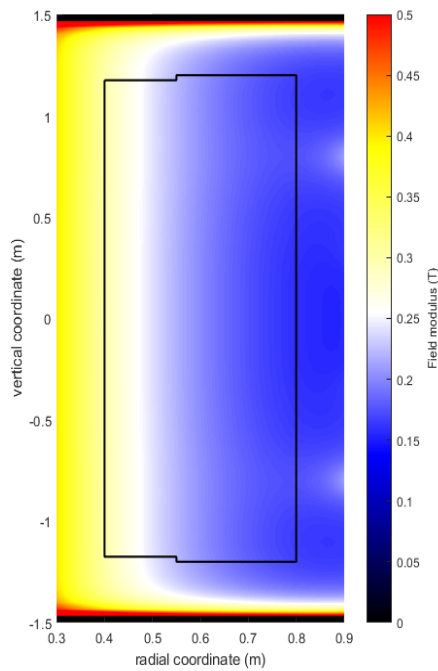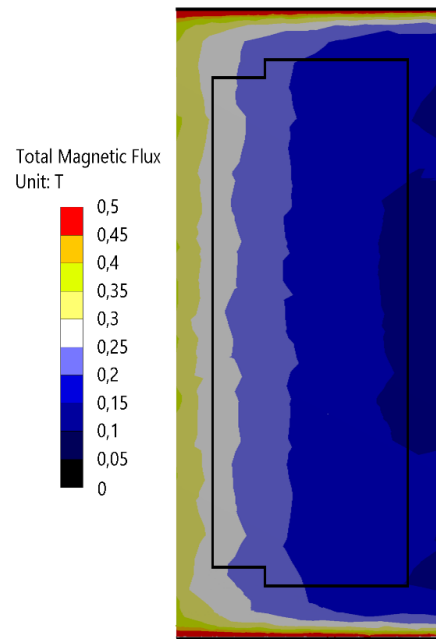
*Figure 44 – Magnetic Field Matlab Results*



*Figure 45 - Magnetic Field Ansys Results*

The results propagation of the Matlab is smoother than in the ANSYS results because of the mesh (much more quality in MATLAB due to the computational limit in ANSYS). Anyway, as we can see in the Figure 44 and Figure 45 the results are very similar which confirm that the calculation in Matlab is correct.

## 3.2   Forces estimation

In this section, we have to use the calculated magnetic field to estimate the forces that it generates. In Matlab, we have a generated mesh that covers the plane where the rectangular coil is located. This mesh has been designed so that some nodes of it coincide perfectly with the segments of the coil, in order to obtain the data of the magnetic field exactly on the position of each segment. The force is calculated according to the Lorentz force law, where only the magnetic terms are taken in account:

$$F = I * \int_a^b \overrightarrow{u_t} \times \vec{B} * dl$$

However, it is impossible to integrate our magnetic field because there is no analytical solution. Anyway, the force can be calculated by discretizing the wires, if we transform the integral into a sum of values using the midpoint rule [6] as an approximation (it is possible because, due to the configuration of the mesh, we have the value of the magnetic field along the whole segment and the different divisions are the elements of the mesh):

$$\int_a^b f(x)\, dx = (b - a) * f\left(\frac{a + b}{2}\right)$$

34

So:

$$F = I * \int_a^b \vec{u_t} \times \vec{B} * dl = I * (b - a) * \vec{B}\left(\frac{a+b}{2}\right)$$

If $a$ and $b$ are the initial and final points of each element of the mesh that matches with the segment. The final force on each segment will be the sum of the force of all the elements of each segment/wire.

After this calculation, we obtain the results of the directional forces applied to the segments/wires of the coils. These forces ($F_x$ in X-axis direction, $F_y$ in Y-axis direction and $F_z$ in Z-axis direction, refer to the Figure 49 for the axis direction) are represented in Figure 46 ($F_x$), Figure 47 (Fy) and Figure 48 ($F_z$). In them, we can see the distribution of the force along the wires dimensionless length (referred to the total length of each wire), from the start point of each of them (0) to the end of them (1):
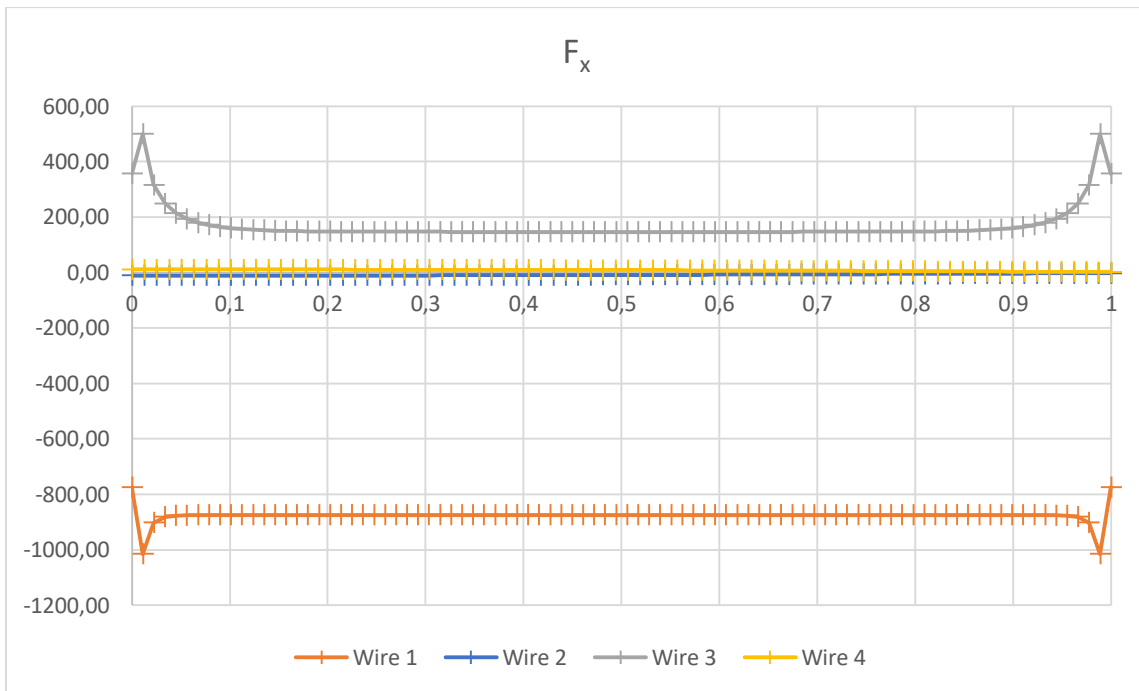


*Figure 46 – $F_x$*

As we can see in Figure 46, there are 2 wires which do not receive force in X-axis direction. They are the numbered as the 2 and the 4 (see Figure 49). It is due to their geometric direction, that is parallel to X-axis (for more info, see Lorentz force law section). On the other ones (1 and 3), it is shown that the biggest value of the forces is on the extremes of the wires, or saying in other way, on the corners of the coils. It is because the magnetic field on this point is ggreater due to the influence of the adjacent wires.
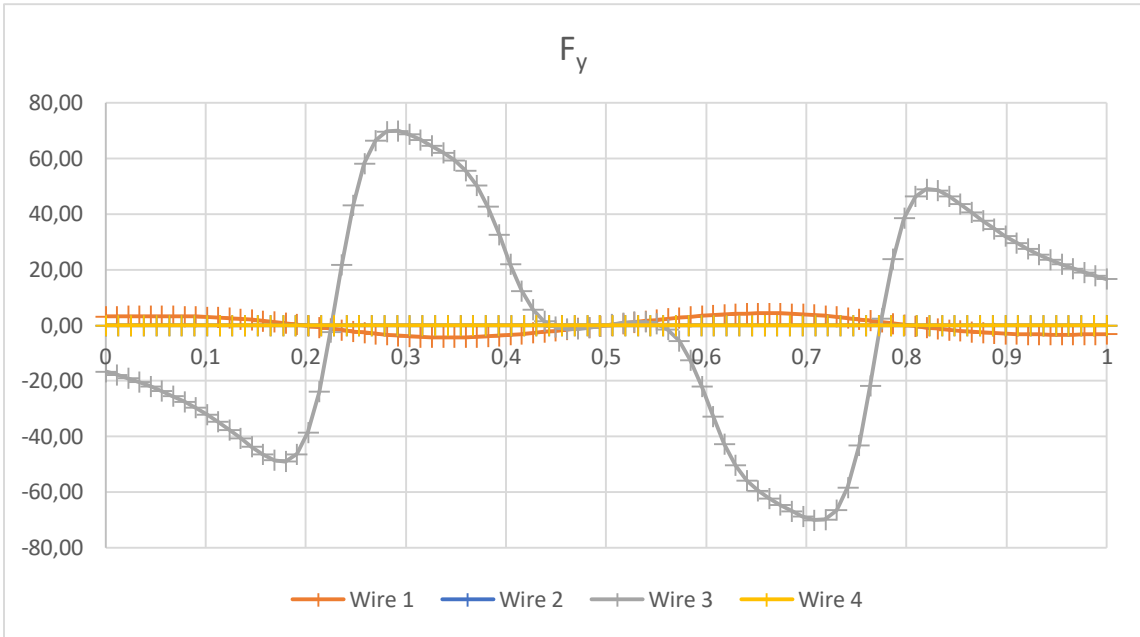
*Figure 47 – $F_y$*

As we can see in Figure 47, the values of the forces in this direction are irrelevant in comparison with $F_x$. This force is not going to be a problem for us and the physic application is that it generates a moment on the coil that will try to force a torsion on the rails along the X-axis.
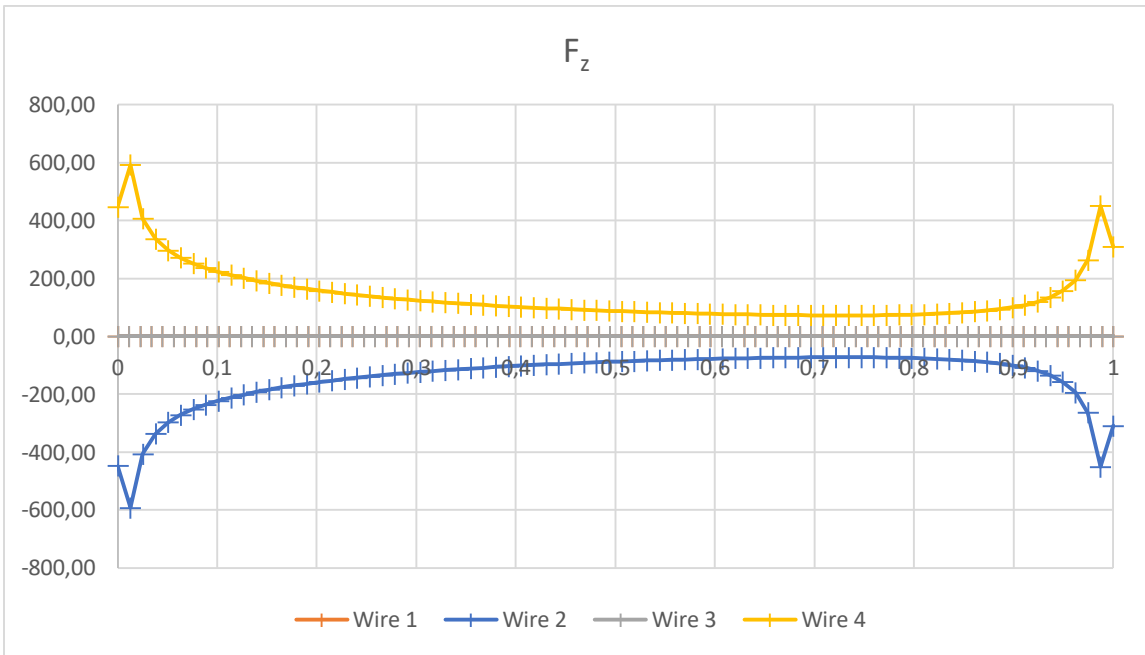


*Figure 48 – $F_z$*

As it is shown in Figure 48, there are 2 wires which do not receive force in this force direction. They are the Wires 1 and 3 (see Figure 49) and this is because of to the direction of them, that is parallel to Z-axis. On the other side, if we analyse the forces on the Wires 2 and 4, we can realize that they are exactly symmetrical.

This last graphic can generate a doubt because in this direction the solution is symmetric, but in the other ones, especially in X-axis, they are not. This is because maybe we have forgotten that the problem is not only a single rectangular coil, we are analysing a complete tokamak and, on the inner side of the tokamak (High Field Side), there are 8 wires together that make that the magnetic field in this area will be greater than far from here (Low Field Side). That reason modifies the $F_x$ in Wire 1 respect from the Wire 3. Furthermore, this effect does not affect to Wires 2 and 4, because they are exactly at the same distance from the centre of the tokamak.

In order to see schematically the forces applied on the wires, see Figure 49:
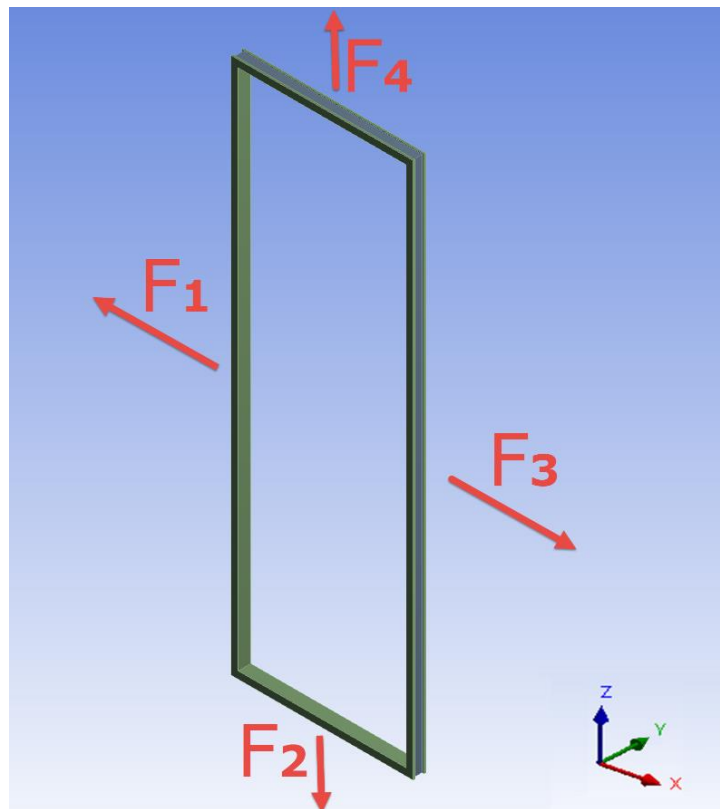


*Figure 49 - Forces Generated*

Where $F_1$ is related to the internal side of the tokamak (High Field Side). The values of the forces is as follow:

- $F_1 = 78903,50 \ N$
- $F_2 = 11416,61 \ N$
- $F_3 = 15371,42 \ N$
- $F_4 = 11416,61 \ N$

As conclusion, the forces generated by the magnetic field attempt to translate the coils to the High Field Side of the Tokamak and expand them in all directions. As the coils are fixed by some supports to the structure of the tokamak, these forces will cause them some certain stresses, stresses that we will have to calculate and design adequate supports that can resist them without working on the limit.

## 3.3 Supports assessment

Now that we have the results of the forces, we can begin with the analysis of the structural integrity of the supports. To do this, the calculated forces are introduced into a FEM model made in ANSYS. If we analyse the components of the forces given in Figure 46 ($F_x$), Figure 47 ($F_y$) and Figure 48 ($F_z$), we can observe that in some situations, the elements of the segments that are together have the same (or very similar) applied force. Thus, for the simulation, these elements have been joined in the model creating some larger ones, and the force applied to them will be the resulting force obtained in Matlab from the elements that made them. The Figure 50 shows how the segments/coils are divided:
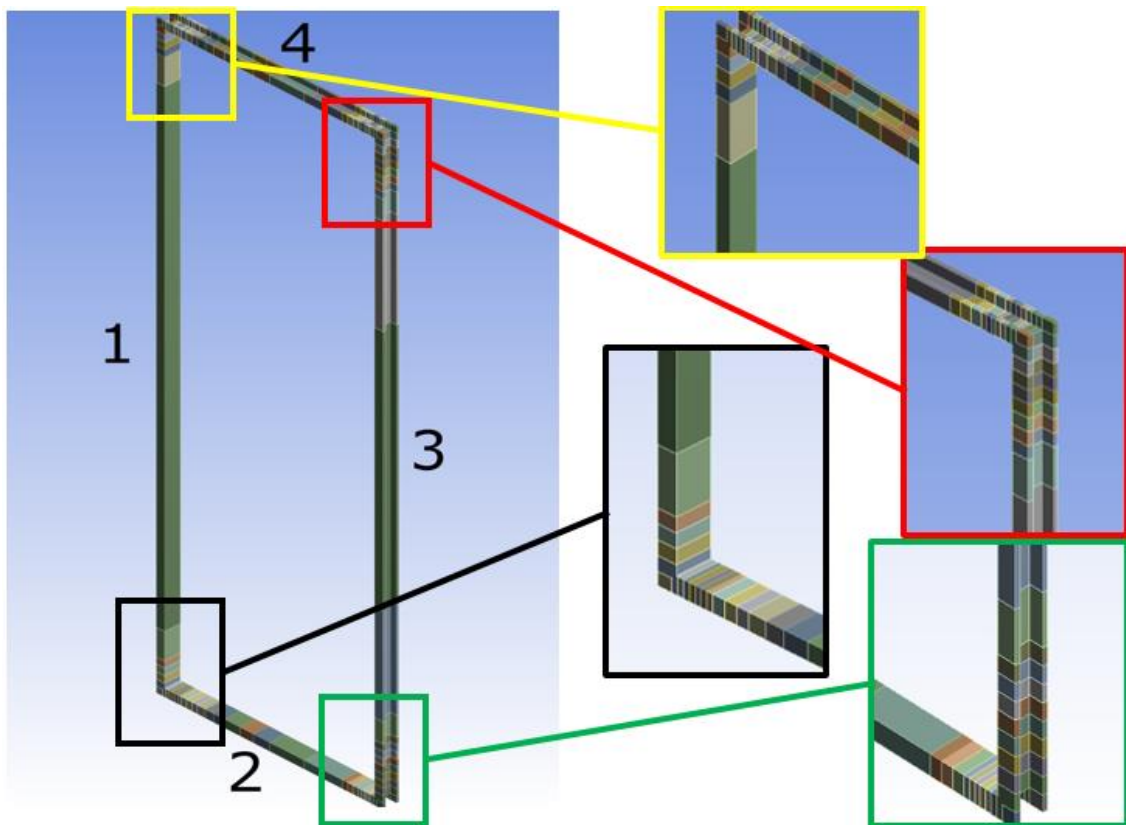


*Figure 50 - Segments Division*

If we analyse it, we can identify that in the vertical wires (1 and 3) the number of final elements is less than in the horizontal ones (2 and 4). It seems logical because the greatest value of the magnetic field will be in the High Field Side (close to the axis of the tokamak) and the variation of the magnetic field will be greater in the direction of X and Y axes than in the Z-axis, because in this case, only horizontal wires and poloidal coils modify the magnetic field.

### 3.3.1  Design of the supports

#### 3.3.1.1  Design

Finally, the aim of this project is to design some supports for the coils that can maintain their position and resist the forces generated without plasticity or breakage. It has been decided that we

are going to create 12 supports, 6 on each side of the rail and distributed in 3 heights along the longest sides, keeping 4 in the centre (2 of them on each side) as shown in Figure 51.
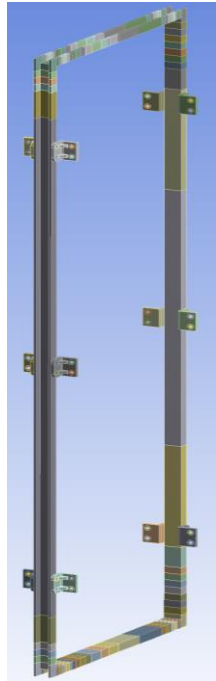


*Figure 51 - Supports Scheme*

We begin with a basic L-profile support (Figure 52) with a hole on each face for one screw each, to attach the support to the rail and the structure. This basic design will be improved to meet the strength requirements.

The initial idea was to use a M12 as a typical industry screw that we thought that could withstand the stresses that will be generated without problems. To simulate the actual installation of the screw, an area surrounding to the hole was modelled to simulate the implementation of a washer (Figure 52), and here the boundary conditions are applied. One of them is to fix them to the ground on the corresponding face (fix support), and the other one is to create a contact region between the area of the washer on the support's face with the rail where the coil is located.
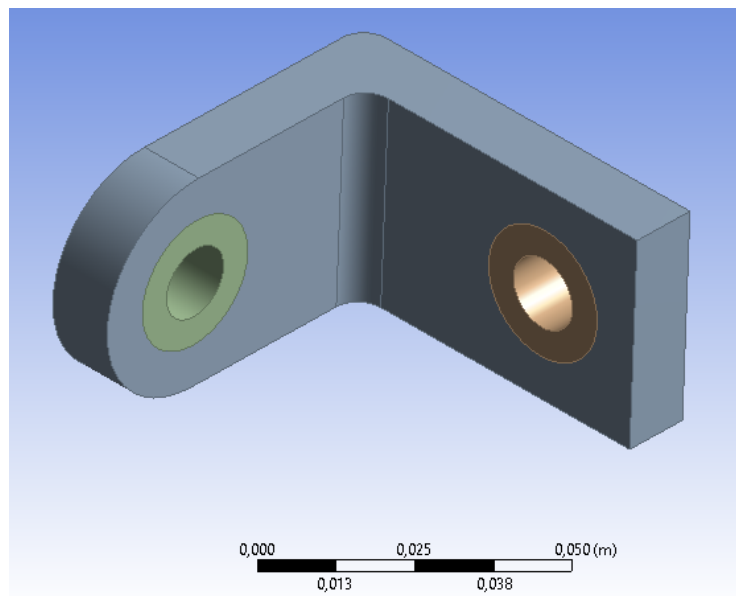


*Figure 52 - Initial Support*

This basic model was not enough to resist all the forces without going through the plasticity state ($\sigma > 270\ MPa$).

The first improvement was to create a reinforcement between the two sides of the L-profile to triangulate the structure, as shown in Figure 53. The idea was to improve the stiffness of the support by reinforcing the stress concentration area (corner):
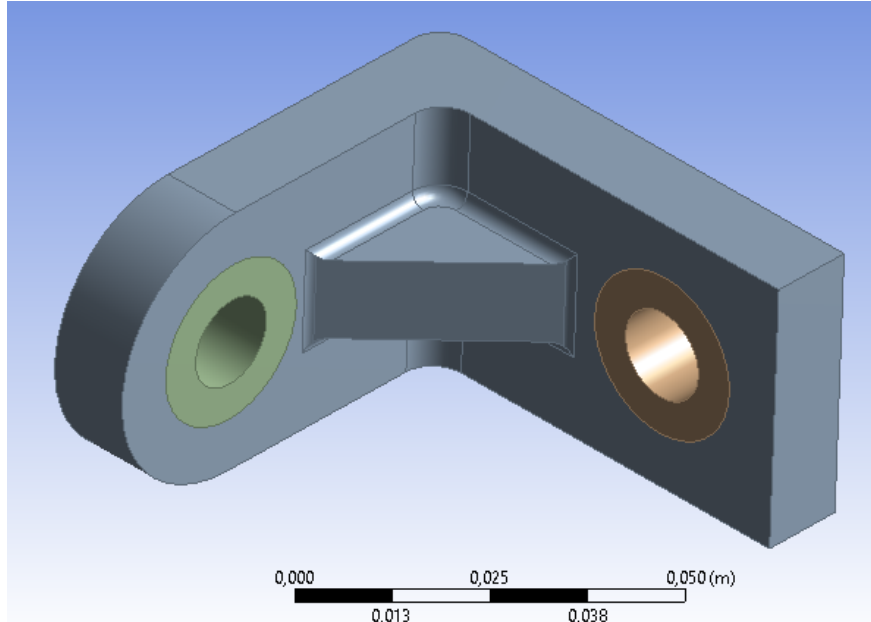


*Figure 53 - Reinforced Support*

The result of this was a reduction in the value of the stress on the support. In this case, if the reinforcement has sufficient width, and the support increases its thickness, we could maintain the support without exceeding the elastic limit ($\sigma = 270\ MPa$), and the maximum values are located in this reinforcement..

However, for this design, we have found a problem with the fasteners. This problem is that the forces applied generate a reaction forces on the screws of the supports that they are not able to withstand.

To solve this, we decide to increase the number of bolts and make a larger support based on the initial idea of an L-profile with 4 holes.

To do this, it is necessary to follow some dimensional rules to determine the distance between holes, as explained below [7]:
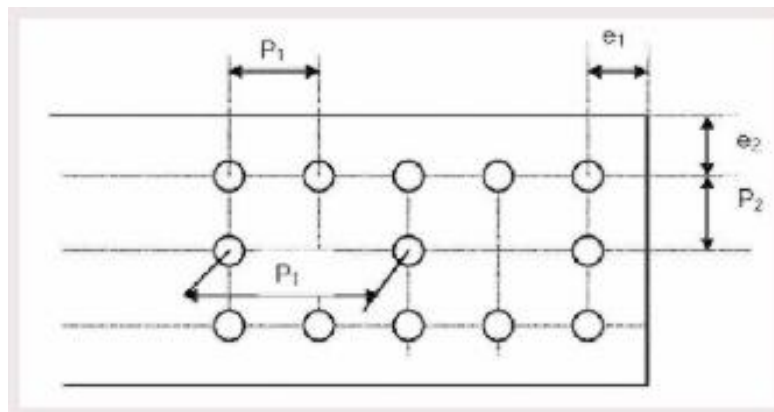


*Figure 54 - Screws Restriction*

$$e_1 \geq 1,2 * d_0$$

$$e_2 \geq 1,5 * d_0$$

$$p_1 \geq 2,2 * d_0$$

Where $d_0$ is the diameter of the hole. In our model:

$$d_0 = 13 \ mm$$

$$e_1 = 20 \ mm \ \geq 15,6 \ mm$$

$$e_2 = \ 20 \ mm \geq 19,5 \ mm$$

$$p_1 = \ 50 \ mm \geq 28,6 \ mm$$

Which defines a new initial model to be improved, shown in Figure 55, which maintains the thickness value of the reinforcement of the previous two holes support.
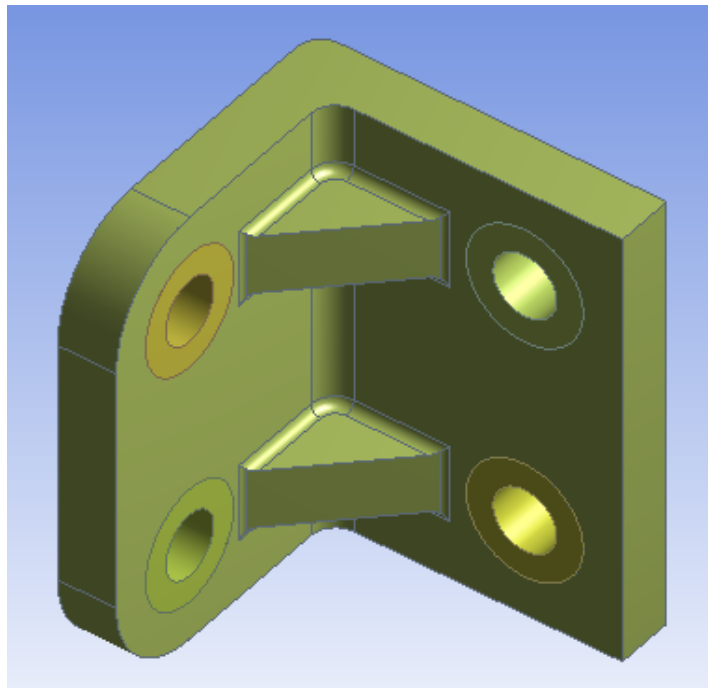


*Figure 55 - Double Reinforced Support*

Once that the new support is simulated, there are two problems:

- a small plasticizing area at the edges of the reinforcement (Figure 56)
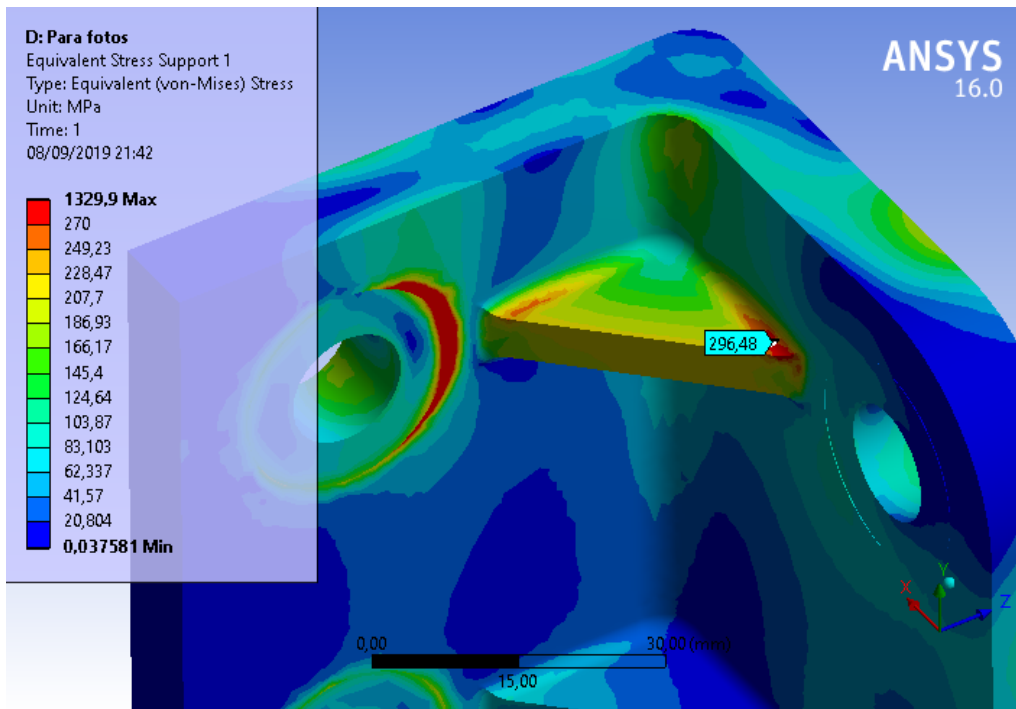- a problem area in the coil's rails (Figure 57)
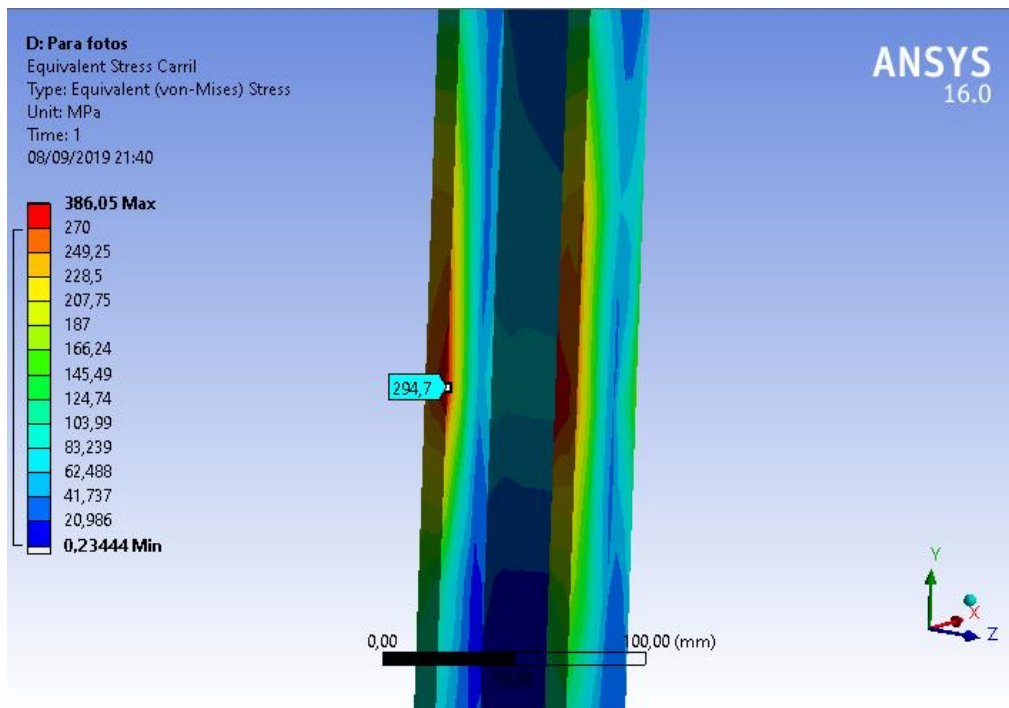
*Figure 56 - Stress Support*



*Figure 57 - Rail Stress*

Apart of this conflict areas, there are some locations where the stresses exceed the maximum value. It occurs on some areas closed to the ones where the boundary conditions have been applied (fixed support and contact area). We have decided to ignore them because they do not show the real performance of the supports and may lead us to think that the support is not worth for the solution.

It is possible to fix both by modifying the position of the supports on the rails, so, if we establish that 4 supports must be fixed in the centre of the rail, we can change the position of the other 8 that are above and below them.

After some iterations, the behaviour of the stress was defined in such a way that as they separate from the centre (where we have fixed 4 supports), there is less stress on the rail, but the stress on the reinforcement increases.

The objective is to obtain a position where the highest point on both of them is below the limit ($\sigma = 270\ MPa$) and the whole model will be satisfactory.

Once we found the position with the best results, we tried to improve the thickness of the support and the reinforcement till the final one of 10 mm for the support and 5 mm for both reinforcements.

The distribution of stress on the most critical supports is shown in Figure 58, Figure 59, Figure 60 and Figure 61:
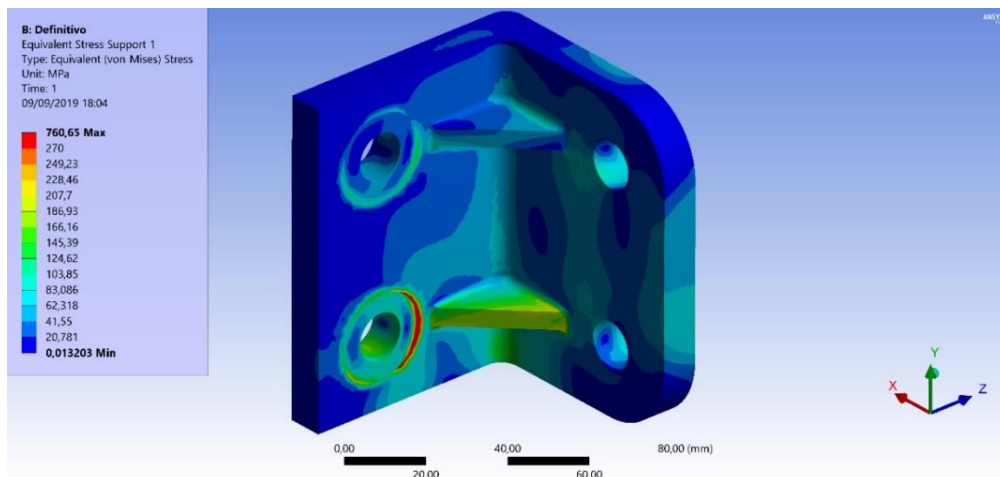


*Figure 58 - Stress Support*



*Figure 59 - Stress Support*
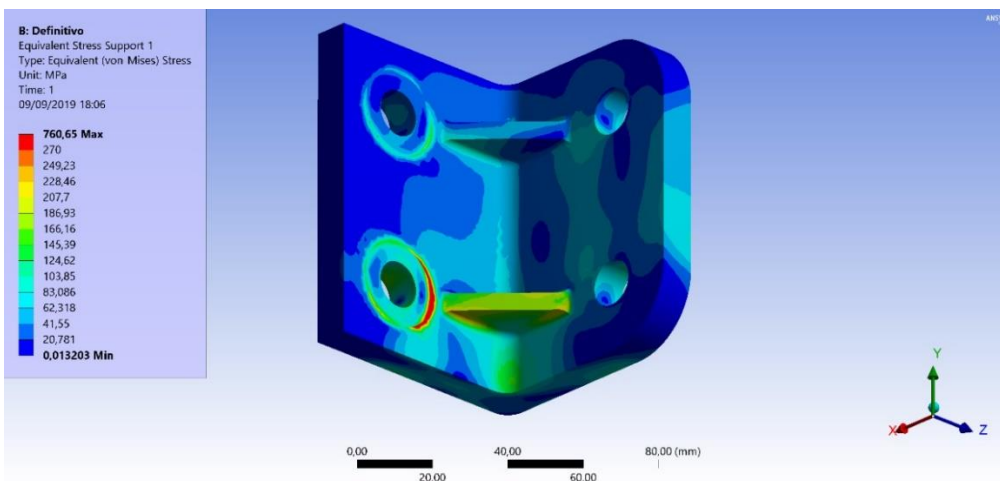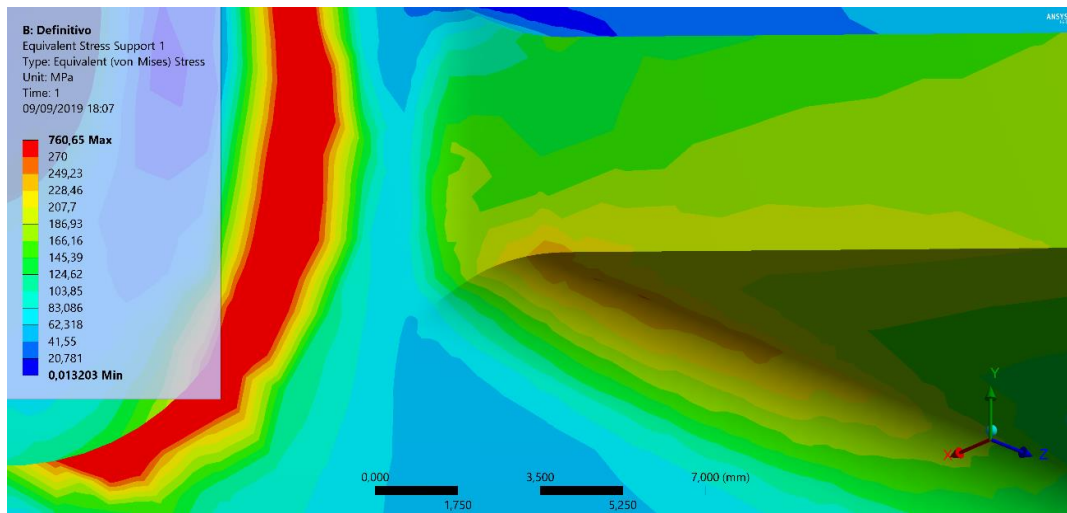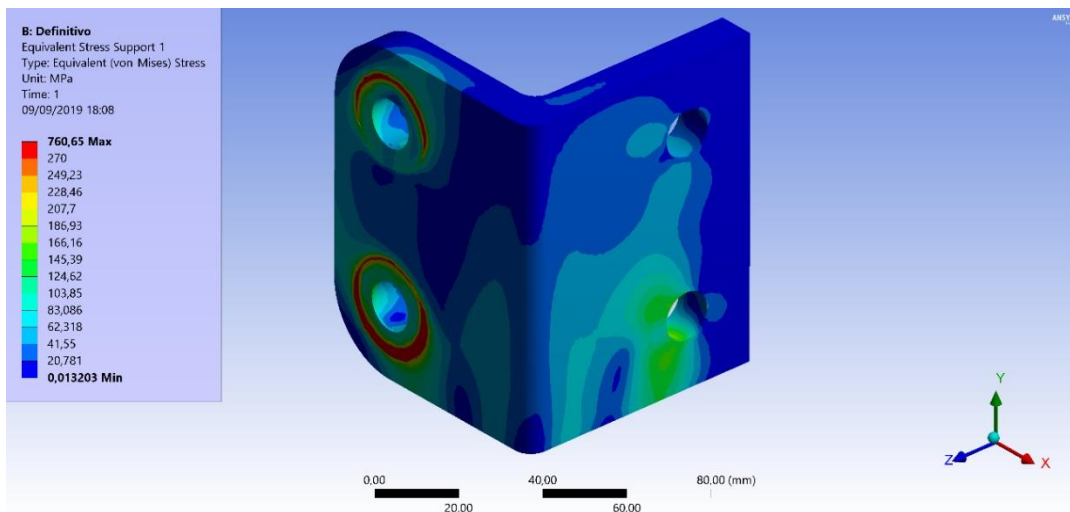
*Figure 60 - Stress Reinforcement Support*



*Figure 61 - Stress Support*

### 3.3.1.2 Fasteners

Once that the supports have been designed to withstand the stresses, we have to check whether the screws can withstand the stresses generated on them.

The result of the simulation gave us the information that the support that received the greatest reaction forces is the one shown in Figure 62:
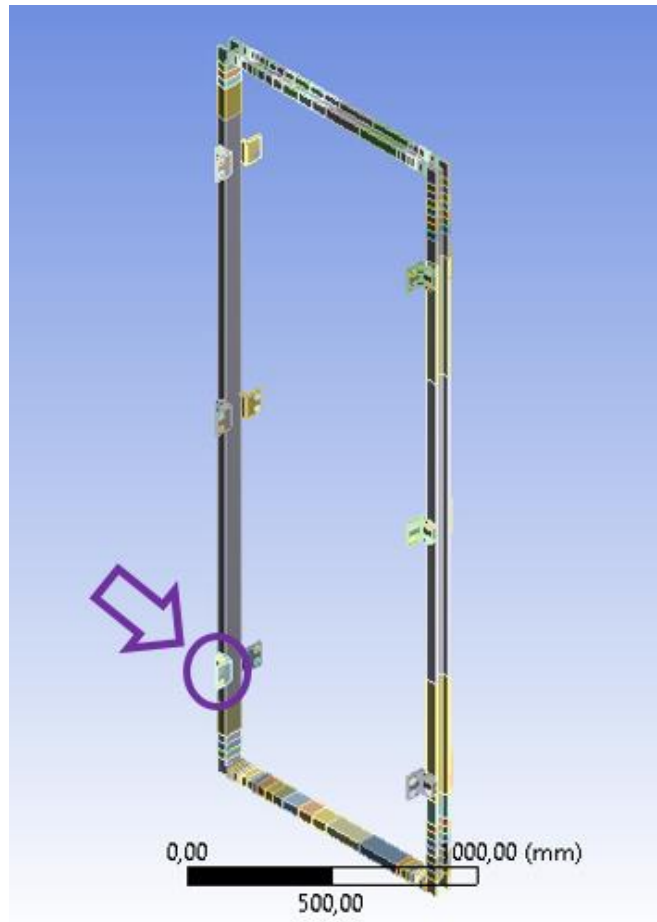
*Figure 62 - Forced Support*

Located in the lower High Field Side of the tokamak. This support has 2 holes which resist the forces shown in Table 2:

|  | Hole 1 | Hole 2 |
|---|---|---|
| Axial force | 6238,5 N | 4458,3 N |
| Shear force | 9808,9 N | 1024,3 N |

*Table 2 – Forces on the Fasteners*

As we can see, the Hole 1 will be the one which need a study to check if the fasteners will resist the stress without problems. For this, we should set some conditions for the bolt and then check some capacities of the junction.

### 3.3.1.2.1 Bolt characteristics

| Category | M12 |
|:---:|:---:|
| $d$ | 12 mm |
| Grade | 8.8 |
| $f_{yb}$ | 640 N/mm² |
| $f_{ub}$ | 800 N/mm² |
| $\gamma_{Mb}$ | 1.25 |
| As | 84.3 mm² |
| d0 | 13 mm |

*Table 3 – Bolt characteristics*

### 3.3.1.2.2 Bolt capacities

To calculate if the bolts will resist [8], we have to begin with the shear resistance:

$$F_{v,Rd} = \frac{0,6 * f_{ub} * A_s}{\gamma_{Mb}} = 64,74 \; KN$$

And the bearing resistance:

$$F_{b,Rd} = \frac{2,5 * \alpha * f_u * d * t}{\gamma_{Mb}}$$

Where:

- $\alpha$ must be the lowest value of:

$$\frac{e_1}{3*d_0} \qquad \text{or} \qquad \frac{p_1}{3*d_0} - \frac{1}{4} \qquad \text{or} \qquad \frac{f_{ub}}{f_u} \qquad \text{or} \qquad 1$$

- $f_u$ is the ultimate tensile strength of the steel of the plate of the support (430 N/mm²)

And then:

$$F_{b,Rd} = \frac{2,5 * \alpha * f_u * d * t}{\gamma_{Mb}} = 52,92 \; KN$$

The tension resistance at ultimate limit states is calculated following the next equation:

$$F_{t,Rd} = \frac{k_2 * f_{ub} * A_s}{\gamma_{Mb}} = 97,11 \; KN$$

Where $k_2 = 0.9$ in our case, because we are not working with countersunk bolts ($k_2 = 0.63$)

The punching shear resistance of the plate is defined as:

$$B_{p,Rd} = \frac{0.6 * \pi * d_m * t * f_u}{\gamma_{Mb}}$$

Where $t$ is the thickness of the plate (10 mm) and $d_m$ is the minimum distance between the nut diameter and the mean value of the bolt head.

Anyway, it is not necessary to calculate de $B_{p,Rd}$ if the thickness (10 mm) of the plate is:

$$t \geq \frac{d * f_{ub}}{6 * f_u} = 3,72 \ mm$$

So, if we compare the resistances calculated we can see that in all cases the bolt can resist the strength which is applied on it:

$$F_{v,Rd} = 64,74 \ KN > F_{v,Ed} = 9,809 \ KN$$

$$F_{b,Rd} = 52,92 \ KN > F_{v,Ed} = 9,809 \ KN$$

$$F_{t,Rd} = 97,11 \ KN > F_{t,Ed} = 6,238 \ KN$$

However, the bolts of the supports of the tokamak are exposed to a mix of shear and tension forces, so they must meet the next condition:

$$\frac{F_{v,Ed}}{F_{v,Rd}} + \frac{F_{t,Ed}}{1,4 * F_{t,Rd}} \leq 1$$

With our parameters:

$$\frac{F_{v,Ed}}{F_{v,Rd}} + \frac{F_{t,Ed}}{1,4 * F_{t,Rd}} = 0,197 \leq 1$$

So, it satisfies the condition, and it has been demonstrated that these M12 bolts are able to resist all the forces required by the tokamak.

# 4 Conclusions and future work

A systematic methodology has been developed for estimating electromagnetic forces acting on the coils of a tokamak. It is a two-step procedure consisting in calculating the magnetic field provided by the energized coils and, after that, estimating the forces generated on the current carrying elements, since they are immersed within a magnetic field. Using these forces, the mechanical assessment of the supporting structures can be faced. Now we can take advantage of this work to continue in some different job areas.

On one hand, starting from this project, this methodology can be applied in future works about magnetism with the related module of ANSYS. Here, it has been shown the reliability of this and where are the limitations that we can find in other projects.

On the other hand, a preliminary design of the tokamak has been set for the initial conditions given and could be developed if the calculation of a vacuum vessel with their covers is done. For this, they must be improved in terms of thickness and shape geometry. Of course, the joint between them must be calculated for the fasteners related. This vacuum vessel could keep the current shape (cylindrical) or it can evolve into other one more similar to the VEST which are 3 cylinders joined.

Another line of improvement could be to change the geometry of the support in order to find an easier/cheaper manufactured shape or other one which could allow to reduce the number of supports in the tokamak.

Also, this work could be used as a reference for further similar methodologies to be developed other FEM computational packages such as COMSOL and ANSYS MAXWELL, widely used within the fusion community.

# 5 References

[1] Plasma start-up design and first plasma experiment in VEST. Seoul National University

[2] Operational Status and Future Plan of VEST. Seoul National University

[3] https://www.electrical4u.com/biot-savart-law/

[4] https://en.wikipedia.org/wiki/Biot%E2%80%93Savart_law

[5] J. Ayllon-Guerola, Private communication

[6] https://en.wikipedia.org/wiki/Mean_value_theorem

[7] https://ingemecanica.com/tutorialsemanal/tutorialn31.html

[8] https://ingemecanica.com/tutorialsemanal/tutorialn32.html